Roles of PSD-93 and environmental enrichment in cortical synapses

Dissertation

in partial fulfilment of the requirements

for the degree

Doctorum rerum naturalium (Dr. rer. Nat.)

in the Molecular Physiology of the Brain Program

at the Georg-August University Göttingen,

Faculty of Biology

submitted by

Plinio Das Neves Favaro

born in

Londrina, Brazil

Göttingen, September 2014

Thesis Committee Members:

Dr. Dr. Oliver M. Schlüter (Reviewer)
Molecular Neurobiology, European Neuroscience Institute, Göttingen

Prof. Dr. Walter Stühmer (Reviewer)
Molecular Biology of Neuronal Signals, Max Planck Institute Experimental Medicine, Göttingen

Prof. Dr. Michael Hörner
Cellular Neurobiology, Johann-Friedrich-Blumenbach-Institute for Zoology and Anthropology, Göttingen

Holger Taschenberger, PhD
Molecular Neurobiology, Max Planck Institute Experimental Medicine, Göttingen

Extended Thesis Committee Members:

Prof. Dr. Siegrid Löwel
Systems Neuroscience, Johann-Friedrich-Blumenbach-Institute for Zoology and Anthropology, Göttingen

Prof. Dr. Nils Bröse
Molecular Neurobiology, Max Planck Institute Experimental Medicine, Göttingen

Day of oral examination: 13th November 2014

Herewith I declare that I prepared the Dissertation "Roles of PSD-93 and environmental enrichment in cortical synapses" on my own and with no other sources and aids than quoted.

Göttingen,   Plinio Das Neves Favaro

Abstract

During neurodevelopment several structural, molecular and functional changes take place in the brain to promote its maturation. These changes occur at multiple levels, including changes in protein expression, in the strength of synaptic transmission and in the susceptibility to experience-driven plasticity.

In the present study, using whole-cell patch-clamp electrophysiology, I examined the roles of PSD-93, a postsynaptic scaffolding protein, in the developmental profile of cortical glutamatergic synapses, in the strength of basal neurotransmission and in the mechanisms of synaptic plasticity. Furthermore, I analyzed how exposure to an enriched environment (EE), with enhanced physical, social and cognitive stimulation, affects both excitatory and inhibitory neurotransmission in the visual cortex of mice.

My results show that, in visual cortex, the normal maturation of glutamatergic neurotransmission was characterized by a robust reduction in the fraction of AMPAR-lacking synapses (silent synapses): from 80% at Postnatal days 3-5 (PD3-5), to about 50% at PD10-12 and further to 25% at PD21-30.

PSD-93 deletion caused accelerated synaptic maturation. The percentage of silent synapses was precociously decreased at PD10-12 (30%), and also at PD21-30 (0%). In depth electrophysiological analysis revealed that this accelerated synaptic maturation, represented by absence of silent synapses at PD21-30, caused a functional increase in the strength of postsynaptic AMPAR neurotransmission, while basal NMDAR function remained normal.

In contrast, PSD-95 deletion prevented synaptic maturation after PD10-12, so the fraction of silent synapses stayed high at PD21-30 (about 50%). Direct comparison of PSD-93 and PSD-95, by simultaneous deletion of both proteins, revealed that the fraction of silent synapses remained indistinguishable from Control at PD21-30. Thus, the present study reveals a novel scenario in which PSD-93 and PSD-95 present opposite roles governing the maturation of glutamatergic neurotransmission.

Furthermore, PSD-93 deletion did not affect basal NMDARs, but impaired NMDAR-dependent LTD, converting it into LTP. This suggests PSD-93 involvement in

coupling NMDAR activity to downstream signaling mechanisms related to synaptic plasticity.

Taken together, these results expand the knowledge about the molecular mechanisms underlying synaptic maturation in visual cortex; and enrich the current view concerning the roles of PSD-93 and its functional interactions regulating synaptic transmission and plasticity.

Concerning EE, it was previously shown that it can increase experience-driven plasticity in the visual cortex, using ocular dominance plasticity (ODP) as a model. Essentially, ODP gradually declines and is absent beyond PD110. However, if mice are raised in EE, ODP is preserved throughout adulthood beyond PD130. In this context, my results show that, beyond PD130, EE mice presented reduced intracortical inhibition when compared to age-matched controls. Furthermore, inhibition levels in old EE mice were indistinguishable from the inhibition levels observed in young mice at PD21-30. Additional results from our collaborators evidenced that the preserved ODP in old EE mice was almost totally abolished by pharmacological boosting of inhibitory neurotransmission.

Thus, the gradual reduction in experience-driven cortical plasticity can be prevented by exposing mice to an enriched environment with enhanced physical, social and cognitive stimulation. The present data show that modulation of intracortical inhibition, by environmental stimulation, plays a key role in this process.

Content

List of Figures

Glossary

aCSF	Artificial cerebrospinal fluid
aEPSC	Asynchronous mEPSC-like response
AMPA	Alpha-amino-3-hydroxyl-5-methyl-4-isoxazole-propionate
AMPAR	Alpha-amino-3-hydroxyl-5-methyl-4-isoxazole-propionate receptor
APV	Amino-5-phosphonovaleric acid
CaMKII	Calcium/Calmodulin kinase II
CB1R	Cannabinoid 1 receptor
CNS	Central Nervous System
DLG-MAGUK	Disc-large membrane-associated guanylate kinase
dNTP	Deoxyribonucleotide
EE	Enriched environment
EGTA	Ethylene glycol tetraacetic acid
EPSC	Excitatory postsynaptic current
GABA	Gamma-aminobutyric acid
HEPES	4-(2-hydroxyethyl)-1-piperazineethanesulfonic acid
IPSC	Inhibitory postsynaptic current
KO	Knock out
L4	Layer 4
L2/3	Layer 2/3

L4-L2/3	Layer 4 to layer 2/3
LTD	Long-term depression
LTP	Long-term potentiation
MD	Monocular deprivation
mEPSC	Miniature excitatory postsynaptic current
mIPSC	Miniature inhibitory postsynaptic current
MK-801	Dizocilpine
NBQX	2,3-dihydroxy-6-nitro-7-sulfamoyl-benzo[f]quinoxaline-2,3-dione
NMDA	N-methyl-D-aspartate
NMDAR	N-methyl-D-aspartate receptor
OD	Ocular dominance
ODP	Ocular dominance plasticity
PCR	Polymerase Chain Reaction
PD	Postnatal day
PDZ	PSD-97/Disc-large/Zona occludens-1
PKA	Protein kinase A
PPR	Paired-Pulse Ratio
Pr	Release probability
PSD	Postsynaptic density
PSD-93	Postsynaptic density protein 93

PSD-95	Postsynaptic density protein 95
SAP-97	Synapse associated protein 97
SAP-102	Synapse associated protein 102
SC	Standard cages
SEM	Standard Error of the Mean
SH3	Src-homology domain 3
shRNA	Short-hairpin RNA
GK	Guanylate kinase
TARP	Transmembrane AMPAR regulatory protein
TEACl	Tetraethylammonium chloride
TTX	Tetrodotoxin
uEPSC	Unitary excitatory postsynaptic current
V1	Primary visual cortex

1 Introduction

Every vertebrate has a central nervous system (CNS) which integrates information from the body and external environment. It plays a critical role coordinating, influencing and generating most aspects of an individual's behavior and physiology.

The CNS is composed by two major parts: the brain and spinal cord. Neurons are the core component of the CNS; they are electrically excitable cells that communicate with one another via their synapses. *Electrical synapses* are direct conductive junctions between two neurons. *Chemical synapses* involve release of neurotransmitters by presynaptic neurons and consequent activation of membrane receptors which drive and modify the activity of postsynaptic cells.

1.1 Synaptic transmission.

Compared to electrical synapses, chemical synapses are the most abundant in the brain. When an action potential reaches the presynaptic terminal, activation of voltage-gated calcium channels at the cell membrane leads to increased calcium levels. Calcium triggers fusion of synaptic vesicles with the presynaptic membrane leading to neurotransmitter release at the synaptic cleft. After release, neurotransmitters diffuse and bind to ionotropic and metabotropic receptors at the postsynaptic membrane.

Ionotropic receptors are ion channels which open following neurotransmitter binding. Ionic current through open channels promotes rapid changes in postsynaptic potentials which can be depolarizing (excitatory) or hyperpolarizing (inhibitory). Excitatory and inhibitory potentials are electrotonically transmitted along the dendritic tree, where their amplitude or time-course can be modulated by voltage-gated ion channels, and finally integrated in the cell body, increasing or decreasing the probability of action potential generation, respectively.

Metabotropic receptors are transmembrane proteins coupled to intracellular metabolic pathways. Their activation does not cause rapid changes in membrane potential, but modifies neuronal metabolism and eventually changes membrane permeability

though modulation of synaptic and non-synaptic ion channels. Thus, metabotropic receptors modulate neuronal functionality.

The action of a neurotransmitter is defined by the kind of postsynaptic receptor it interacts with. Excitatory, inhibitory and modulatory neurotransmitters activate cation channels, anion channels and metabotropic channels, respectively. In the brain, excitatory neurotransmission is primarily mediated by glutamate, inhibitory neurotransmission by GABA; and modulatory neurotransmission by a number of transmitters, including serotonin, dopamine and others.

1.1.1   Glutamatergic synaptic transmission.

Glutamate is the major excitatory neurotransmitter in the brain. Its fast excitatory function is mediated by three types of postsynaptic cationic receptors: AMPA receptors (AMPARs), NMDA receptors (NMDARs) and kainate receptors. In addition, glutamate presents an alternative modulatory role activating G-protein coupled metabotropic receptors. AMPARs and NMDARs are the main ionotropic glutamate receptors and the focus of the present study.

1.1.1.1   AMPA receptors.

AMPARs mediate the vast majority of information flow in the brain. AMPARs are tetramers of the subunits GluA1-GluA4. The different subunits bind to distinct interacting partners, differentially modulate AMPAR trafficking and control the ionic conductance of single-channels (Malinow and Malenka, 2002; Bredt and Nicoll, 2003).

Each subunit contains a glutamate-binding site (Mayer, 2005). When two subunits are simultaneously activated by glutamate, the channel opens allowing cations to flow according to their electrochemical gradients (Rosenmund et al, 1998). In case additional subunits are activated, single-channel conductance increases (Armstrong et al, 2006). The intracellular C-terminus of GluA1 is longer when compared to GluA2 subunits. It is suggested that trafficking of GluA1 subunits to synaptic sites is activity-dependent and relies on NMDAR activation. In contrast, trafficking of GluA2 subunits appears to be

constitutive and receptors containing this subunit mediate basal AMPAR neurotransmission (Hayashi et al, 2000; Passafaro et al, 2001).

GluA2 subunits render AMPARs calcium impermeable. In contrast, GluA2-lacking AMPARs are permeable to calcium and pass less current at positive potentials due to voltage-dependent block by intracellular polyamines. In addition, given its calcium conductance, GluA2-lacking AMPARs are suggested to play a role in activating downstream signaling pathways which can potentially modulate postsynaptic mechanisms (Wiltigen et al, 2010).

1.1.1.2 NMDA receptors.

NMDARs are tetramers of four subunits: GluN1-4 (Nakanishi, 1992; Hollmann and Heinemann, 1994). They are permeable to calcium, sodium and potassium. Most NMDARs are composed of two obligatory GluN1 and two GluN2 subunits. GluN1 subunits contain the binding site of co-agonists glycine and D-serine. GluN2 subunits contain the binding site for glutamate, render NMDAR calcium permeable and control channel activity mediating its blockade by extracellular magnesium at negative potentials (Mayer and Armstrong, 2004).

In general, GluN2B subunits are predominantly expressed in early postnatal development. However, during maturation, GluN2A subunits are gradually added to the synapses, exceeding the number of GluN2B subunits (Liu et al, 2004). In addition, GluN2A-containing NMDAR excitatory postsynaptic currents (EPSCs) present faster decay time when compared to GluN2B-containing NMDAR EPSCs.

NMDARs are coincidence detectors. Their activation requires simultaneous release of glutamate and postsynaptic depolarization. When these two conditions are established, NMDARs are relieved of magnesium block and ionic flow takes place through the channel (Mayer et al, 1984; Nowak et al, 1984).

The complexities of NMDAR-associated signaling are a topic of intense interest, given its involvement in mechanisms as diverse as neuronal plasticity, neurodevelopment, learning and disease (Paoleti et al, 2013). Efficient functional coupling between NMDARs and specific intracellular signaling pathways, instead of mere receptor activation, appears to be the key feature determining how NMDAR-mediated calcium

influx governs neuronal plasticity and development (Sattler et al, 1999). As an example, deletion of PSD-95 (a scaffolding protein in excitatory synapses) disrupts NMDAR-dependent synaptic plasticity but has no effect on basal NMDAR EPSCs (Beique et al, 2006; Migaud et al, 1998; Carlisle et al, 2008). Therefore, the identification of molecular players specifically linking NMDARs with intracellular signaling pathways will enrich the current knowledge about NMDAR function and the mechanisms it is involved with, such as synaptic plasticity, neurodevelopment and learning (Paoletti et al, 2013).

1.1.1.3   NMDAR-dependent synaptic plasticity.

Synaptic plasticity is the ability of synapses to strengthen or weaken in response to changes in their activity (Hughes, 1958). Several mechanisms are involved, including changes in the efficiency of postsynaptic response or alterations in neurotransmitter release. Long-term potentiation (LTP) and long-term depression (LTD) refer to synaptic strengthening and weakening, respectively. Synaptic plasticity is suggested to be a key brain mechanism underlying learning, memory and proper network refinement during development (Katz and Shatz, 1996).

NMDAR-dependent forms of synaptic plasticity were described in different brain regions (Bliss and Gardner-Medwin, 1973; Artola et al, 1996; Tsien et al, 1996). They can be induced by specific patterns of synaptic stimulation or by selective activation of distinct NMDAR subpopulations (Hrabetova et al, 2000).

In NMDAR-dependent LTP, activation of NMDARs, by concomitant pre- and postsynaptic activity, leads to high intracellular calcium levels. In general, synaptic strengthening requires activation of calcium/calmodulin kinase II (CaMKII) and insertion of AMPARs at postsynaptic sites. (Malinow et al, 1989; Malenka et al, 1989; Giese et al, 1998). Therefore, NMDAR-dependent LTP is achieved by increases in postsynaptic response to glutamate.

Concerning NMDAR-LTD, NMDAR activation can lead to protein kinase A (PKA) activation and clathrin-dependent endocytosis of postsynaptic AMPARs (Crozier et al, 2007). Additionally, it is suggested that endocannabinoids released by the postsynaptic neuron, in a calcium dependent manner, can diffuse along the synaptic cleft to activate presynaptic cannabinoid 1 receptors (CB1Rs) and induce LTD via reduction of

glutamate release (Sjöstrom et al, 2003). Therefore, NMDAR-dependent LTD can be achieved by decreased postsynaptic response or by reduction in neurotransmitter release.

The functional coupling between NMDARs and the signaling mechanisms related to LTP and LTD is puzzling. Despite their opposite effects on synaptic transmission, both LTP and LTD are triggered by NMDAR activation. Identification of the molecular players specifically linking NMDARs to signaling pathways related to LTD or LTP, and their differential recruitment by different patterns of synaptic activity, consists a key step required to clarify this scenario.

In addition, the lesser studied NMDAR-independent forms of synaptic plasticity can be mediated by metabotropic glutamate receptors, calcium permeable AMPARs and other calcium permeable channels (Kullman and Lansa, 2011).

1.1.2 GABAergic synaptic transmission.

Gamma-aminobutyric acid (GABA) is the main inhibitory neurotransmitter in the brain. It activates two membrane receptors: $GABA_A$, an ion channel; and $GABA_B$, a G-protein coupled metabotropic receptor.

1.1.2.1 GABA$_A$ receptors.

$GABA_A$ receptors mediate most of the physiological activities of GABA. Upon activation, $GABA_A$ receptors open allowing flow of chloride to the intracellular compartment. The resulting hyperpolarization has an inhibitory influence decreasing the probability of actions potential to occur.

$GABA_A$ are pentamers composed of different subunits. In humans there are six types of α subunits, three βs, three γs, one δ, one ε, one π and one θ. Both α and β subunits are required to produce a GABA-activated channel and the most common $GABA_A$ receptors are composed by two α subunits, two βs and one γ. GABA binding sites are located at the interfaces between α and β subunits, thus the most common $GABA_A$ receptors present two binding sites for GABA (Martin and Dunn, 2002; Colquhoun and Sivilotti, 2004).

Neurons that produce and release GABA are, in general, small locally-projecting interneurons They are key elements organizing neuronal networks to generate rhythmic activity, and play a critical role modulating the glutamatergic influence on local microcircuits (Freund, 2003; McBain and Fisahn, 2001). Exceptions to this rule are the spiny medium neurons in basal ganglia or inhibitory neurons in zona incerta (Lin et al, 1990).

1.2   DLG-MAGUKs.

Glutamate receptors at the postsynaptic membrane are part of an electron-dense protein-enriched complex known as postsynaptic density (PSD). The PSD controls the trafficking of glutamate receptors and allows proper modifications in synaptic strength during synaptic plasticity. DLG-MAGUKs (disc-large membrane-associated guanylate kinases) are four different scaffolding proteins expressed at the PSD: PSD-93 (postsynaptic density protein 93), PSD-95, SAP-97 (synapse associated protein 97) and SAP-102.

All DLG-MAGUKs share a common molecular structure. They consist of three PDZ (PSD-97/Disc-large/Zona occludens-1) domains, one Src-homology 3 (SH3) domain and one guanylate kinase (GK) domain which is catalytically inactive. Despite their common structure, DLG-MAGUKs are distinct concerning the aminoacid sequence of their N-terminal domains, which can present unique functions (Schlüter et al, 2006)

PSD-93, PSD-95 and SAP-102 interact with AMPARs via transmembrane AMPAR regulatory proteins (TARPs). TARPs bind to both MAGUKs and AMPARs. SAP-97 is the only MAGUK which directly binds to AMPARs at their GluA1 subunits (Leonard et al, 1998). In contrast, all MAGUKs directly interact with GluN2A and GluN2B NMDAR subunits (Kornau et al, 1995; Niethammer et al, 1996). The ability to interact with both AMPARs and NMDARs suggests that MAGUKs can be central players regulating the trafficking of glutamate receptors and orchestrating the functional organization of the PSD.

SAP-97 Knock out (KO) is lethal. However, SAP-97 deletion in conditional KO mice was reported to cause no major impact on basal glutamatergic neurotransmission and plasticity (Howard et al, 2010). SAP-97 overexpression is reported to increase

(Rumbaugh et al, 2003; Howard et al, 2010), or have no impact on postsynaptic AMPARs (Schnell et al, 2002; Erlich and Malinow, 2004; Schlüter et al, 2006).

SAP-102 deletion decreases AMPAR neurotransmission specifically at immature synapses (Elias et al, 2006). In the mature state, basal neurotransmission is normal but NMDAR-dependent LTP enhanced in the absence of SAP-102 (Cuthbert et al, 2007). Additionally, SAP-102 can have a compensatory role counteracting the loss of synaptic AMPARs caused by PSD-95 deletion (Elias et al, 2006; Bonnet et al, 2013). The last two MAGUKs, PSD-93 and PSD-95, will be introduced in the following sections.

1.2.1 PSD-95.

PSD-95 is the most abundant and better characterized DLG-MAGUK. Concerning NMDARs, PSD-95 might play a role mediating the switch of GluN2B to GluN2A subunits during normal synaptic maturation. However, PSD-95 deletion has no impact on basal NMDAR neurotransmission at mature synapses. Concerning AMPARs, PSD-95 levels are directly related to the strength of AMPAR neurotransmission. PSD-95 deletion and overexpression leads to decreased and increased AMPAR function, respectively (Elias et al, 2006; Nakagawa et al 2004; Schlüter et al, 2006).

Changes in the number of silent synapses are a crucial point defining PSD-95 roles of AMPAR neurotransmission. It is known that some synapses contain functional postsynaptic NMDARs but not AMPARs. Therefore, at resting membrane potential, neurotransmitter release fails to elicit EPSCs in these synapses and for this reason they are considered to be silent (Isaac et al, 1995; Liao et al, 1995). In general, changes in the fraction of silent synapses are electrophysiologically characterized by modified AMPAR miniature EPSC (mEPSC) frequency. mEPSCs are postsynaptic responses to single spontaneously released synaptic vesicles. Changes in AMPAR mEPSC amplitude reflect changes in AMPAR number or single-channel conductance at existing synapses. Changes in AMPAR mEPSC frequency reflect changes in presynaptic release of glutamate or changes in the fraction of silent synapses. High and low fraction of silent synapses cause decreased or increased mEPSC frequency, respectively.

Manipulations of PSD-95 levels modify the frequency, but not amplitude, of spontaneous miniature AMPAR EPSCs (mEPSCs), without changing glutamate release.

It is suggested that PSD-95 promotes insertion and stabilization of AMPARs at silent synapses leading to increased AMPAR mEPSC frequency. On the other hand, PSD-95 deletion decreases the strength of AMPAR neurotransmission by increasing the number of silent synapses. (Stein et al, 2003, Beique and Andrade, 2003, Beique et al, 2006).

Furthermore, PSD-95 deletion leads to enhanced LTP and blocked LTD, while PSD-95 overexpression has exactly the opposite effect (Migaud et al, 1998; Stein et al, 2003). This suggests that PSD-95 has a role modulating NMDAR-dependent trafficking of AMPARs to synaptic sites (Xu et al, 2008), an idea further reinforced by the direct interaction between PSD-95 and NMDARs.

1.2.2   PSD-93.

Information about PSD-93 is limited when compared to PSD-95.

In cerebellum, PSD-93 appears to have no major effect on synaptic transmission and associated motor behavior (McGee et al, 2001). However, PSD-93 deletion decreases cell-surface expression of NMDARs in forebrain and spinal cord (Tao et al, 2003; Liaw et al, 2008), and reduces NMDAR-mediated toxicity in cortical cultures (Zhang et al, 2010). In contrast, AMPARs are reported to be unaffected in the aforementioned brain areas.

In hippocampus the scenario is different. According to Elias et al (2006), PSD-93 deletion reduces AMPAR neurotransmission in organotypic cultures, evidencing a redundant role when compared to PSD-95. However, genetic PSD-93 Knockout has minor or no influence on basal AMPAR neurotransmission in this brain region (Carlisle et al, 2008; Krüger et al, 2013). Furthermore, the relationship between PSD-93 levels and the number of silent synapses was not addressed. While it is a consensus that basal NMDAR function is normal, PSD-93 deletion causes deficits in NMDAR-dependent LTP, but not in LTD (Carlisle et al, 2008). In contrast, as commented earlier, PSD-95 deletion has an opposite effect enhancing LTP and blocking LTD (Beique et al, 2006; Migaud et al, 1998; Carlisle et al, 2008). It is unclear why PSD-93 and PSD-95 have opposite roles in synaptic plasticity but apparently redundant functions on basal AMPAR neurotransmission. Additional direct comparisons between these two MAGUKs are essential to solve this question.

Furthermore, as exposed in the previous paragraph, PSD-93 function might depend on a multiplicity of different factors including the synapses and brain region under analysis. In contrast, PSD-95 appears to have similar roles on neurotransmission irrespective of brain region. Thus, region-specific PSD-93 functions consist another important issue which needs to be better clarified.

1.2.3 Developmental profile of DLG-MAGUKs.

DLG-MAGUKs present distinct developmental profiles in rodents. SAP-102 reaches its highest levels at postnatal day 10 (PD10), consistent with its critical role regulating AMPARs at immature synapses (Sans et al, 2000). SAP-97 is already expressed at birth and reaches adult levels around PD14 (Wang et al, 2006). PSD-93 and PSD-95 are poorly expressed at birth, but their levels start to increase around PD10, reaching adult levels around PD35 (Sans et al, 2000). Thus, given their differential expression profiles, the relative importance of MAGUKs can vary depending on the developmental stage at which synaptic transmission and plasticity are analyzed.

However, an in depth analysis of the functional interplay between MAGUKs regulating the development of NMDAR and AMPAR neurotransmission, including PSD-93, is not available. This is an important topic which might reveal that different scaffolds can differentially regulate neurotransmission depending on the developmental stage, and also play distinct roles governing synaptic maturation.

1.3 Visual cortex.

The visual system of rodents and other mammals present many similarities. Visual information from retina is transmitted as action potentials, via the optic nerve, to the lateral geniculate nucleus in the thalamus and further to primary visual cortex (V1).

For each eye, fibers from medial retina cross to the contralateral hemisphere at the optic chiasm, before reaching the lateral geniculate nucleus. In contrast, fibers from the lateral retina do not cross and, therefore, send information to the ipsilateral hemisphere. As a result, fibers from the left part of retina of both eyes send visual information to the

left hemisphere and vice-versa. Since stimuli from the right visual field activate the left part of retina, each hemisphere receives information from the contralateral visual field.

Visual stimulation presented to the contralateral eye evokes stronger responses in neurons at V1 when compared to similar stimulation presented to the ipsilateral eye. Thus, V1 neurons are primarily activated by visual stimuli of the contralateral eye, a condition referred to as contralateral ocular dominance (OD) (Dräger 1975; Mangini and Pearlman 1980; Wagor et al. 1980; Metin et al. 1988). Closing the contralateral eye of a mouse for a few days causes neurons in V1 to respond almost equally to visual stimuli presented to each eye. Thus, OD shifts in favor of the open eye. This process is known as ocular dominance plasticity (ODP) and is one of the most studied forms of brain plasticity (Dräger, 1975; Gordon and Stryker, 1996; Espinosa and Stryker, 2012).

1.3.1   Age-dependent ODP in visual cortex.

In neurodevelopment, *critical period* is a time frame in which greater shaping and plasticity of neuronal networks can be carried out. In mice, ODP has greater magnitude around PD19-PD32 during the so called *critical period* for ODP. This form of brain plasticity gradually declines and is absent beyond PD110 if animals are raised in standard cages (SC) (Lehmann and Löwel 2008). The neuronal factors underlying this age-dependent decline are not completely understood. If rodents are housed in an enriched environment (EE) with enhanced cognitive, physical and social stimulation, ODP is preserved throughout adulthood and can be successfully induced after PD130 (Baroncelli et al, 2010; Scali et al, 2012). Intracortical levels of inhibition appear to play a key role, as extracellular GABA levels are reduced in the visual cortex of EE rodents (Sale et al, 2007). Moreover, by increasing $GABA_A$ activity with the allosteric agonist diazepam, the preserved ODP of EE rodents can be completely blocked (Baroncelli et al, 2010).

Despite the aforementioned evidence suggesting inhibitory tone to play a critical role in regulating the expression of ODP, the integrity of GABAergic synaptic transmission was not evaluated by direct measurement of $GABA_A$ inhibitory postsynaptic currents (IPSCs) in cortical neurons of EE-mice.

In addition to increased inhibitory tone, several other factors are suggested to play a role in reducing and abolishing ODP in PD>110 mice. These factors include reduced

function of modulatory neurotransmitters (Maya Vetencourt et al, 2008; Morishita et al, 2010), maturation of structural elements of the extracellular matrix (Carulli et al, 2010; Miyata et al, 2012) and myelination (Syken et al, 2006).

1.3.2 Molecular mechanisms of ODP in visual cortex.

The ODP induced by 4 days of monocular deprivation, during the critical period (PD19-PD32), is characterized by reduced responsiveness of the contralateral V1 to visual stimuli presented to the deprived eye. NMDAR-dependent LTD at cortical glutamatergic synapses was suggested to be the key synaptic mechanism underlying this form of experience-dependent brain plasticity. This notion is supported by several studies. Intracortical infusion of NMDAR antagonist APV disrupts ODP in juvenile individuals (Kleinschmidt et al, 1987; Bear et al, 1990), NMDAR-dependent LTD is maximum during the critical period and decreases with age (Kirkwood et al, 1997; Sermasi et al, 1999), and NMDAR-dependent LTD, studied *ex vivo*, is occluded in the deprived visual cortex (Crozier et al, 2007). It is suggested that prior synaptic depression *in vivo* during ODP occludes subsequent induction of LTD *ex vivo* in acute brain slices (Heynen et al, 2003).

In contrast, several other studies failed to show a direct relation between NMDAR-dependent LTD and ODP. For example, overexpression of calcineurin has no effect on NMDAR-dependent LTD but prevents ODP in mice (Yang et al., 2005). Furthermore, autophosphorylation of αCaMKII is necessary for ODP (Taha et al., 2002), but not for LTD (Giese et al., 1998). In addition, recent studies suggest that reduction in V1 responsiveness to the deprived eye is achieved through modulation of intracortical inhibition (Yazaki-Sugiyama et al, 2009).

Therefore, it appears that ODP is not solely mediated by NMDAR-dependent LTD. Further studies are necessary to better elucidate the additional mechanisms employed by the brain during this form of experience-driven plasticity.

1.4   Scope of this thesis

1.4.1   PSD-93 roles in synaptic transmission.

Glutamate receptors at the postsynaptic membrane are part of an electron-dense protein-enriched complex known as postsynaptic density (PSD). The PSD controls the trafficking of glutamate receptors and allows proper modifications in synaptic strength during synaptic plasticity. PSD-95 is the prototypical scaffolding protein at the PSD. Essentially, PSD-95 levels are directly related to the strength of AMPAR neurotransmission. PSD-95 deletion and overexpression are reported to decrease and increase AMPAR function, respectively (Elias et al, 2006; Nakagawa et al 2004; Schlüter et al, 2006). Furthermore, PSD-95 regulates AMPAR neurotransmission by modulating the number of AMPAR-lacking silent synapses (Stein et al, 2003, Beique and Andrade, 2003, Beique et al, 2006). PSD-93 was suggested to have a similar role, when compared to PSD-95, in hippocampus (Elias et al, 2006). However, additional studies failed to show the same effect of PSD-93 deletion reducing AMPAR neurotransmission (Carlisle et al, 2008). Furthermore, it is not known whether PSD-93 influences the number of silent synapses, as suggested for PSD-95.

Concerning other brain regions, PSD-93 deletion was reported to decrease NMDAR cell-surface expression in forebrain and spinal cord (Tao et al, 2003; Liaw et al, 2008), and to reduce NMDAR-mediated toxicity in cortical cultures (Zhang et al, 2010), while AMPARs were apparently unaffected. However, synaptic receptors were not specifically evaluated. Thus, further analyses of PSD-93 in synapses from different brain regions are necessary, considering its potential region-dependent roles differentially governing AMPARs and NMDARs.

In the present study, PSD-93 roles were specifically evaluated during synaptic development of the visual cortex, between PD3-5 and PD21-30. The objective was to dissect how and when PSD-93 starts to govern basal neurotransmission in the time-course of normal cortical neurodevelopment. In visual cortex, the fraction of silent synapses gradually decreases during development (Rumpel et al, 1998, 2004). Therefore, a direct comparison between PSD-93 and PSD-95 roles regulating the fraction and maturation of silent synapses was carried out. The objective was to establish the functional interplay

between these two scaffolds. Are they really similar concerning basal neurotransmission? How do they functionally interact to maintain the integrity of glutamatergic synapses and normal synaptic maturation?

Furthermore, PSD-93 roles on basal synaptic AMPARs and NMDARs were evaluated in detail using a combination of different electrophysiological approaches, in order to verify how the previously reported changes in global NMDAR cell-surface expression relate specifically to synaptic receptors. Is PSD-93 deletion really reducing NMDAR neurotransmission? Is it possible that PSD-93 differentially regulate synaptic and extra synaptic NMDARs? What about synaptic AMPARs?

Finally, the implications of NMDAR basal neurotransmission and PSD-93 for NMDAR-dependent plasticity were evaluated. What's the critical factor governing NMDAR-dependent synaptic plasticity? Basal NMDAR function? The functional coupling between NMDARs and intracellular signaling pathways? What's the role of PSD-93 in this context?

By addressing the aforementioned questions, knowledge about the molecular mechanisms underlying synaptic maturation in visual cortex will be expanded. Additionally, it will enrich the current view concerning the roles of PSD-93 and PSD-95 and their functional interactions governing synaptic transmission and plasticity.

Therefore, using a combination of whole-cell patch-clamp electrophysiology, transgenic mice and viral mediated knockdown of endogenous DLG-MAGUKs *in vivo*; the present study aims to define the specific role of PSD-93 on AMPAR and NMDAR neurotransmission and NMDAR-dependent plasticity in cortical synapses.

1.4.2 Synaptic changes induced by Environmental Enrichment.

In primary visual cortex (V1), neurons are primarily activated by visual stimuli of the contralateral eye, a condition referred to as contralateral ocular dominance (OD) (Dräger 1975; Mangini and Pearlman 1980; Wagor et al. 1980; Metin et al. 1988). Closing the contralateral eye for a few days makes neurons in V1 respond similarly to visual stimuli presented to each eye. This is known as ocular dominance plasticity (ODP) and is one of the most studied forms of brain plasticity (Dräger, 1975; Gordon and Stryker, 1996; Espinosa and Stryker, 2012).

ODP gradually declines and is absent beyond PD110 if mice are raised in standard cages (SC) (Lehmann and Löwel 2008). However, if rodents are housed in an enriched environment (EE) with enhanced cognitive, physical and social stimulation, ODP is preserved throughout adulthood (Baroncelli et al, 2010; Scali et al, 2012). Intracortical levels of inhibition appear to play a key role, as extracellular GABA levels are reduced in the visual cortex of adult EE rodents (Sale et al, 2007). Moreover, by increasing $GABA_A$ activity with the allosteric agonist diazepam, the preserved ODP of EE rodents can be completely blocked (Baroncelli et al, 2010).

Despite the aforementioned evidence suggesting inhibitory tone to play a critical role in regulating the expression of ODP, the integrity of GABAergic synaptic transmission was not evaluated by direct measurement of $GABA_A$ IPSCs in cortical neurons of EE-rodents. Furthermore, it is not known whether excitatory synapses were additionally affected.

Therefore, using *ex vivo* whole-cell patch-clamp electrophysiology, the present study aims to define how GABAergic neurotransmission changes during normal maturation of V1, and how EE affects this process. Does GABAergic neurotransmission increase between initial stages of development and adulthood to reduce ODP? Does EE inhibit this process? What about glutamateric neurotransmission? Does EE have an additional effect of AMPAR and NMDAR EPSCs? Elucidation of these questions will determine how EE influences synaptic transmission in V1 and enhance our knowledge about which factors facilitate the experience-driven ODP.

2 Materials and Methods

2.1 Mice and housing conditions.

Mice were bred in standard conditions (12-h light/dark cycle). Food and water were available *ad libitum*. PSD-93 KO, PSD-95 KO, PSD-93/95 double-KO and wild-type mice were weaned at PD20. After weaning, males and females were housed in separated cages.

2.1.1 Housing at enriched environment.

C57BL/6J mice were raised by Dr. Franziska Greifzu. For reference see Greifzu et al. (2014). One week before delivery, pregnant females were placed in commercially available enriched environment (EE) cages (Marlau, Viewpoint, France). Pups, born in EE or standard cages (SC), were weaned at PD30 and males separated from females.

EE-cages (56x37x32cm) were larger than standard cages (SC; 26x20x14cm). Each EE-cage contained three running wheels and a red tunnel in which mice could protect themselves from light exposure. The two floors in each EE-cage were connected by a ladder and a tube, so animals could freely move up and down. In order to obtain food and water, mice had to pass through a maze in the upper floor and, after that, move to the lower floor where food and water were available. The maze was changed 3 times each week, from a total of 12 different possible configurations. To ensure a social enrichment condition (up to 16 animals in each EE cage), mice from at least 2-3 litters were raised together. In contrast, fewer mice were kept together in standard cages. Mice raised in EE or SC were used for patch-clamp experiments.

2.2   Genotyping.

2.2.1   Genotyping of PSD-93 KO mice.

The PSD-93 Knockout (KO) mouse line was described by McGee et al, 2001. Genotype was defined through Polymerase Chain Reaction (PCR) of DNA obtained from 1-2 mm tail pieces of each mouse. Tails were digested for at least 3 hours in PBND buffer (150 µl, 55 °C, constant shaking). Once digestion was complete, the proteinase K present in the PBND buffer was inactivated at 99°C for 10 min. For each PCR 2 µl of lysate were used:

PCR mix: PCR program:

2.2 µl   10X TNK buffer   Time/Temp

2 µl   dNTP mix (Bioline)   5' 94°C   initialization

0.2 µl   Primer (PSD-93intron)   45'' 94°C   denaturation

0,2 µl   Primer (PSD-93exon-n2)   1' 61°C   annealing   } x35

0.2 µl   Primer (PSD-93neo)   2' 72°C   elongation

15 µl H_2O 10' 72°C   extention

0.2 µl   MangoTaq Polymerase (Bioline)

2 µl   Lysate

PCR products from wild-type and PSD-93 KO alleles have, respectively, 330 base pairs and 750 base pairs. Bands were separated by horizontal electrophoresis (120V for 35 min in 1% sodium tetraborate agarose gel), and visualized using an UV-illuminator with INTAS imaging system.

Primers:

Primer (PSD-93intron): GTGCGGAATGTTGTTGTGCAGTGC

Primer (PSD-93exon-n2): CACAACAGTCTCCAATATGGGTCGC

Primer (PSD-93neo): GCCTTCTATCGACTTCTTGACGAG

Solutions:

PBND buffer: 10mM Tris, 50mM KCl, 2.5mM $MgCl_2.6H_2O$, 0.1 mg/ml gelatine, 0.45% (v/v) Nonident P40, 0.45% (v/v) Tween 20, 1.2 mg/ml proteinase K, pH 8.3.

10X TNK buffer: 100mM Tris, 15mM $MgCl_2$, 500mM KCl, 50mM NH_4Cl.

1% agarose sodium tetraborate gel: 1% agarose, 5mM sodium tetraborate decahydrate, 15μl/L of ethidium bromide 1%.

2.2.2   Genotyping of PSD-93/PSD-95 double-KO mice.

PSD-93/PSD-95 double-KO mice used were generated in our animal facility by systematic crossing of PSD-93 KO and PSD-95 KO mice. PSD-93 genotype was defined as described in section 2.2.1. PSD-95 genotype was defined as described in section 2.2.1 with the following modifications:

PCR mix: PCR program:

2.2 μl	10X TNK buffer	Time/Temp	
2 μl	dNTP mix (Bioline)	5' 94°C	initialization
0.2 μl	Primer 1	45'' 94°C	denaturation
0,2 μl	Primer 2	45'' 55°C	annealing
15.2 μl	H_2O	1' 72°C	elongation
0.2 μl	MangoTaq Polymerase (Bioline)	10' 72°C	extention
2 μl	Lysate		

} x35 (denaturation / annealing)

PCR products from wild-type and PSD-95 KO alleles have, respectively, 255 base pairs and 355 base pairs. Bands were separated by horizontal electrophoresis (120V for 45 min in 1% sodium tetraborate agarose gel).

Primers:

Primer 1: CAGGTGCTGCTGGAAGAAGG.

Primer 2: CTACCCTGTGATCCAGAGCTG.

2.3   Virus preparation and *in vivo* injections into the visual cortex of newborn mice.

A shRNA construct to knockdown endogenous PSD-95 was prepared as described previously (Schlüter et al, 2006). The shRNA construct was under the control of a CAG promoter in an adeno-associated viral vector. Viruses were produced as described before (Suska et al, 2013).

In order to further evaluate the role of endogenous PSD-95 on the developmental profile of silent synapses in PSD-93 KO mice, *in vivo* injections were carried out by Dr. Xiaojie Huang (European Neuroscience Institute Göttingen, Germany). Briefly, PSD-93 KO newborn mice (PD0-PD2) were anesthetized on ice (10 min) and immobilized in a home made holder under the binocular. A glass capillary, filled with a high titer large-scale virus solution containing the shRNA construct against endogenous PSD-95, was coupled to a Nanoject II microinjector. The thin skin of newborns allowed visual identification of the injection site. The tip of the capillary was placed just above the visual cortex, at a 90° angle, and a quick move of the microinjector pierced both the skin and the skull. The capillary tip was placed 1 mm deep in the brain and viruses were delivered to each hemisphere. After injection, the capillary was slowly removed and animals kept on a heating plate (30°C) until recovery from anesthesia. At the end of the procedure mice were returned to their home cages. At PD10-PD12 or PD21-PD30, acute brain slices were prepared for electrophysiological recordings.

2.4   Preparation of acute brain slices.

Coronal brain slices (400 μm), containing the primary visual cortex, were prepared from SC, EE, wild-type, PSD-93 KO and PSD-93/PSD-95 double-KO mice. Animals were deeply anesthetized with isoflurane and decapitated. The brain was rapidly removed in ice-cold sucrose cutting buffer (composition in μM: sucrose, 204; KCl, 2.5; $MgSO_4$, 4; NaH_2PO_4, 1; $NaHCO_3$, 26; D-(+)-glucose, 10; and $CaCl_2$, 1, bubbled with 95% O_2/5% CO_2 [pH 7.4]). Slices were cut on a vibrating microtome (Leica VT-1200S),

recovered in artificial cerebrospinal fluid (aCSF): (composition in mM: NaCl, 119; KCl, 2.5; $MgSO_4$, 1.3; NaH_2PO_4, 1; $NaHCO_3$, 26; D-(+)-glucose, 20; and $CaCl_2$, 2.5, bubbled with 95% O_2/5% CO_2) at 35°C for 20-30min, and stored at room temperature until use (1–7 h).

2.5 Electrophysiology.

Whole-cell patch-clamp recordings were performed in layer 2/3 pyramidal neurons, visually identified with an infrared-differential interference contrast microscope (Zeiss, examiner D1). Acute slices were placed in a recording chamber continuously perfused with aCSF (29±2°C) at 1-2ml/min rate. In voltage-clamp experiments, patch pipettes (3–6 MΩ) were filled with (in mM): cesium gluconate, 120-130; HEPES, 20; EGTA, 0.4; NaCl, 2.8; TEACl, 5; MgATP, 4; NaGTP, 0.3; and adjusted to pH 7.2-7.3 with CsOH (285-290 mOsm). For current-clamp experiments, patch pipettes were filled with (in mM): potassium gluconate, 116; KCl, 6; NaCl, 2; HEPES, 20; EGTA, 0.5; MgATP, 4; NaGTP, 0.3; adjusted to pH 7.2-3 with KOH (300 mOsm).

Pipette capacitance was minimized in all recordings. Series and input resistance were continuously monitored and the liquid junction potential not corrected. Data were acquired at 10 kHz and filtered at 3 kHz using an ELC-03XS patch-clamp amplifier (npi, electronic instruments for the life sciences, Germany). For analysis, custom routines in Igor (Wavemetrics, Lake Oswego, OR) and Minianalysis (Synaptosoft, Fort Lee, NJ) s were used.

2.5.1 Intrinsic excitability.

Input resistance and resting membrane potential were measured immediately after obtaining current-clamp configuration. Intrinsic excitability was assessed by measuring the number of action potentials triggered by current steps applied to the pipette (in pA): 50, 75, 100, 125, 150, 175, 200, 225, 250, 275 and 300. Each current step had a fixed duration of 500 ms.

2.5.2 Basal synaptic transmission.

Synaptic transmission was recorded with voltage-clamp electrophysiology. In all experiments aCSF contained 50μM picrotoxin to block inhibition, unless otherwise specified.

2.5.2.1 Spontaneous synaptic events.

Spontaneous miniature Excitatory Post-Synaptic Currents (mEPSCs) were recorded in aCSF supplemented with TTX 1μM. Membrane voltage was -70mV and, for each neuron, 400 mEPSCs were analysed.

2.5.2.2 Synaptic events evoked by electrical stimulation.

A concentric bipolar stimulating electrode was placed in layer IV and evoked synaptic events were recorded from layer II/III pyramidal cells. Excitatory and inhibitory postsynaptic currents (EPSCs and IPSCs, respectively) were evoked at a constant rate of 0.2-0.12Hz.

To estimate the percentage of silent synapses in visual cortex a "failure analysis of minimal EPSCs" was used. Minimal EPSCs were obtained by adjusting the electric stimulus to evoke a combination of postsynaptic responses and failures. For each experiment 50-60 sweeps at -60mV and +40mV were recorded. Percentage of silent synapses was calculated with the following equation: $1- LN(F_{-60})/LN(F_{+40})$. F_{-60} and F_{+40} represent failure rates of minimal EPSCs at -60mv and +40mV, respectively.

For the AMPA/NMDA ratio protocol, AMPAR EPSCs were calculated by averaging 30 EPSCs at −60mV and measuring the peak (0.5ms window) compared to the baseline (10ms window). NMDAR EPSCs were calculated by averaging 30 EPSCs at +40mV and measuring the amplitude (0.5ms window) 60ms after the EPSC peak to ensure the absence of AMPAR component.

To obtain rectification index of AMPARs, 20 EPSCs were recorded at -70mV, -50mV, -30mV, -10mV, +10mV, +30mV and +50mV. NMDAR EPSCs were blocked by APV 50μM and the internal solution contained spermine 100μM.

Recording of asynchronous EPSCs (aEPSCs) was performed at -70mV in a modified aCSF containing $SrCl_2$ 8mM and no $CaCl_2$.

For GABA/AMPA ratio recordings, aCSF contained no picrotoxin and was supplemented with APV 50μM, to block NMDAR EPSCs. AMPAR EPSCs were calculated by averaging the peak of 30 EPSCs at -70mV (equilibrium potential for GABAR IPSCs), and GABAR IPSCs were calculated by averaging the peak of 30 IPSCs at +5mV (reversal potential for AMPAR EPSCs).

2.5.3 Synaptic plasticity.

Long-Term Depression (LTD) of AMPAR EPSCs was induced in acute slices. After 10 minutes of stable baseline recording at -65 mV, LTD was triggered by pairing presynaptic stimulation with postsynaptic depolarization to -45mV (100ms). Pairings were at a constant rate of 1Hz for 5 min. A modified aCSF containing $CaCl_2$ 2.0mM, $MgSO_4$ 1.0mM and picrotoxin 10μM was used. Cells with stable series and input resistance were considered for analysis.

2.6 Statistical analysis.

Intra and inter-group comparisons were analyzed by two-tailed t-test with Bonferroni correction. Spontaneous AMPAR miniature EPSCs were analyzed with Kormogorov-Smirnov test. Significance was set at $p < 0.05$. Data is presented as mean ± Standard Error of the Mean (SEM).

3 Roles of PSD-93 in synaptic transmission

3.1 Selective increase of AMPAR to NMDAR EPSCs in the absence of PSD-93.

In order to evaluate whether endogenous PSD-93 plays a role governing the strength of basal glutamatergic neurotransmission at L4-L2/3 synapses, voltage-clamp electrophysiology was used to record AMPAR and NMDAR EPSCs in acute brain slices from PSD-93 KO mice.

The ratio of AMPAR EPSCs to NMDAR EPSCs (AMPA/NMDA ratio) is a standard approach to detect postsynaptic changes that differentially modulate AMPAR and NMDAR function (Crair and Malenka, 1995; Carroll et al, 2001, Beique et al, 2006). In this context, PSD-93 deletion selectively increased AMPAR to NMDAR EPSCs at L4/L2-3 synapses (Fig 3.1; Control, 1.64 ± 0.19 [neurons/mice {n/m} = 11/3]; PSD-93 KO, 2.57 ± 0.17 [n/m = 13/4]; $p<0.05$ t-test).

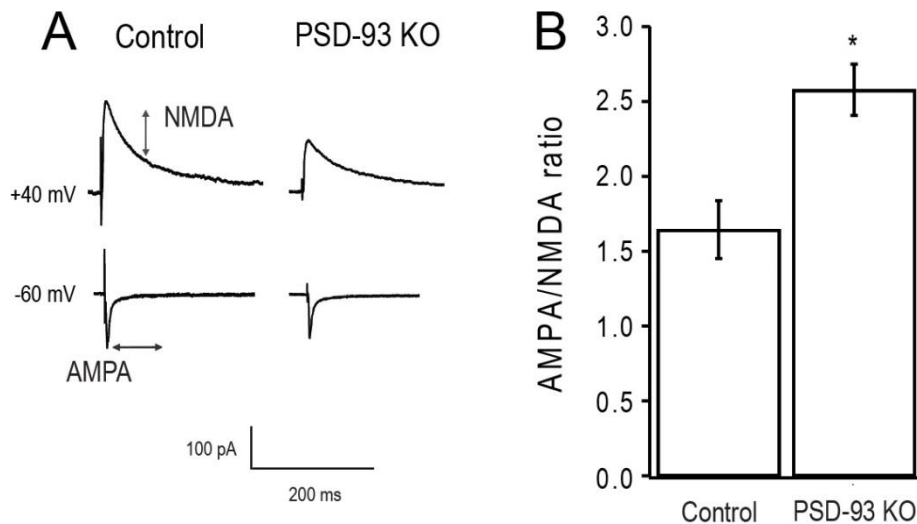**Figure 3. 1: Increased AMPA/NMDA ratio in the absence of PSD -93.**

A: Sample average traces of AMPA/NMDA ratio recordings in Control and PSD-93 KO slices at PD21-30. AMPAR EPSC is the peak value at -60 mV; late NMDAR EPSC was recorded 60 ms after AMPAR peak, at +40 mV. **B**: Summary bar graph of AMPA/NMDA ratio results (Control vs. PSD-93 KO, $p<0.05$ t-test). Inhibition was blocked by picrotoxin 50μM.

Increased AMPA/NMDA ratio can be the result of increased AMPAR or decreased NMDAR function. Previous works reported that PSD-93 deletion decreases NMDAR cell-surface expression in spinal cord and forebrain (Tao et al, 2003; Liaw et al, 2008), and reduces NMDAR-mediated toxicity in cortical cultures (Zhang et al, 2010). In contrast, AMPARs were unaffected. Authors from the above mentioned studies suggested that synaptic NMDARs might be decreased in the absence of PSD-93. An idea apparently supported by the increased AMPA/NMDA ratio observed in spinal cord cultures from PSD-93 KO mice (Tao et al, 2003).

3.2   Roles of PSD-93 in regulating synaptic NMDARs.

In order to analyze the integrity of synaptic NMDARs specifically in L4-L2/3 synapses of visual cortex, two electrophysiological approaches were used: recording of unitary NMDAR EPSCs and pharmacological evaluation of NMDAR subunit composition.

3.2.1   Normal unitary NMDAR EPSC amplitude in the absence of PSD-93.

To obtain unitary L4-L2/3 NMDA responses (uEPSCs), a bipolar stimulating electrode was placed in L4 and L2/3 neurons were voltage-clamped at +40 mV. In each recording, stimulation intensity was slowly increased until the smallest evoked EPSC, here defined as uEPSC, could be identified. Once this condition was obtained, 60-100 sweeps were recorded. The weak presynaptic stimulation caused a combination of postsynaptic responses (uEPSCs) and failures. Presumably, uEPSCs are putative single axon evoked EPSCs from axons in L4 to L2/3 pyramidal neurons (Fig. 3.2).

NMDAR uEPSC recordings are technically demanding. Isolated NMDAR uEPSCs do not present a sharp onset, as observed for AMPAR uEPSCs (see section 3.7), rendering them more difficult to be identified. In addition, neurons voltage-clamped at +40 mV present lower input resistance, increased noise level and generally less stable baseline when compared to -70mV. Combination of the above mentioned factors complicate the recording and analysis of NMDAR uEPSCs. Therefore, special procedures were used to analyze the data.
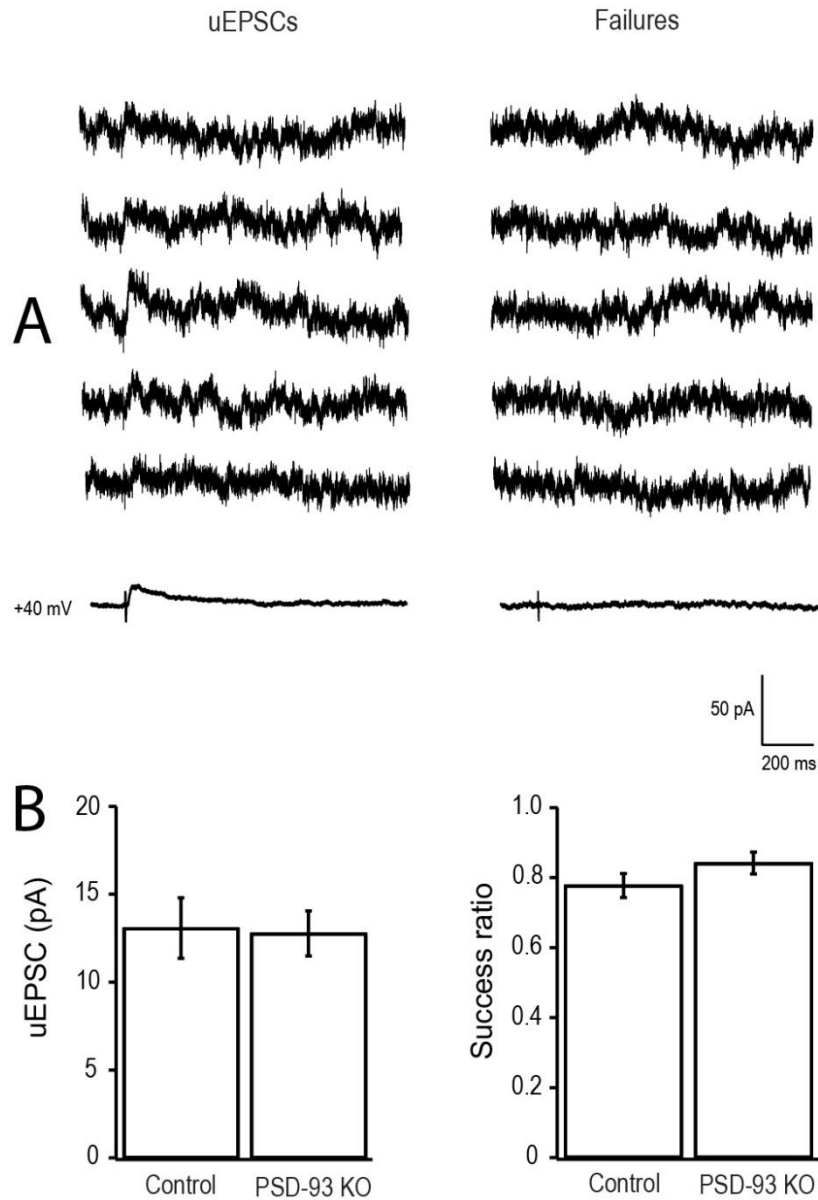
uEPSCs　　　　　　　　　Failures

A

+40 mV

50 pA

200 ms

B

Figure 3. 2: Normal NMDAR uEPSC in the absence of PSD-93.

A: Sample traces of NMDAR uEPSCs (top left) and synaptic failures (top right) from a Control slice. Average trace of identified NMDA uEPSCs evidencing an outward synaptic current (down left). Average trace of synaptic failures consisting of a straight line (down right). AMPARs were blocked by NBQX 5µM and inhibition blocked by picrotoxin 50µM**B**: Summary bar graphs showing that PSD-93 deletion causes no change on NMDAR uEPSC amplitude (left; Control vs. PSD-93 KO, $p>0.05$, t-test), or NMDA uEPSC Success ratio (right; Control vs. PSD-93 KO, $p>0.05$, t-test). Data presented as mean ± SEM.

For each recording, synaptic responses and failures were manually separated by the experimenter during analysis. Sweeps containing responses and sweeps containing failures were averaged separately. The averaged trace of failures consists of a straight line; the averaged trace of responses is characterized by a small outward deflection, the NMDAR uEPSC (Fig 3.2A). Amplitudes of NMDAR uEPSCs were systematically measured 15-20 ms after extracellular stimulation.

NMDAR uEPSC amplitude at L4-L2/3 synapses appears to be normal in the absence of PSD-93 (Fig 3.2B; Control, 13.08 pA ± 1.72 [n/m = 12/3]; PSD-93 KO, 12.77 pA ± 1.28 [n/m = 13/3]; p = 0.88, t-test). As mentioned, in uEPSC recordings a fraction of presynaptic stimulations fails to elicit detectable EPSCs. Success ratio was defined as the number of detected uEPSCs divided by the total number of presynaptic stimulations. Consistent with no change in NMDAR uEPSC amplitude, PSD-93 deletion did not affect the success ratio of evoked NMDAR uEPSCs (Fig. 3.2B; Control, 0.78 ± 0.03 [n/m = 12/3]; PSD-93 KO, 0.84 ± 0.03 [n/m = 13/3], p>0.05, t-test).

3.2.2   Normal NMDAR subunit composition in the absence of PSD-93.

To further analyze the role of PSD-93 in regulating NMDAR neurotransmission, a pharmacological approach was used to evaluate NMDAR subunit composition in PSD-93 KO slices.

NMDARs are tetramers composed of four subunits (Nakanishi, 1992; Hollmann and Heinemann, 1994). Each NMDAR contains two GluN1 subunits combined with GluN2A and/or GluN2B subunits, resulting in the formation of di- or tri-heteromeric receptors. The GluN2B subunit is predominantly expressed in early postnatal development. However, during maturation, GluN2A subunits are gradually added to the synapses, exceeding the number of GluN2B subunits.

Isolated NMDAR EPSCs were recorded at +40mV. After 5 min of stable baseline, GluN2B containing NMDARs were selectively blocked by wash in of Ifenprodil 3μM. The fractional block of NMDAR EPSCs by ifenprodil was not affected by PSD-93 deletion (Fig. 3.3; Control, 0.77 ± 0.08 [n/m = 9/3]; PSD-93 KO, 0.80 ± 0.05 [n/m = 6/3]; p = 0.69, t-test), suggesting normal NMDAR subunit composition in synapses of PSD-93 KO slices.
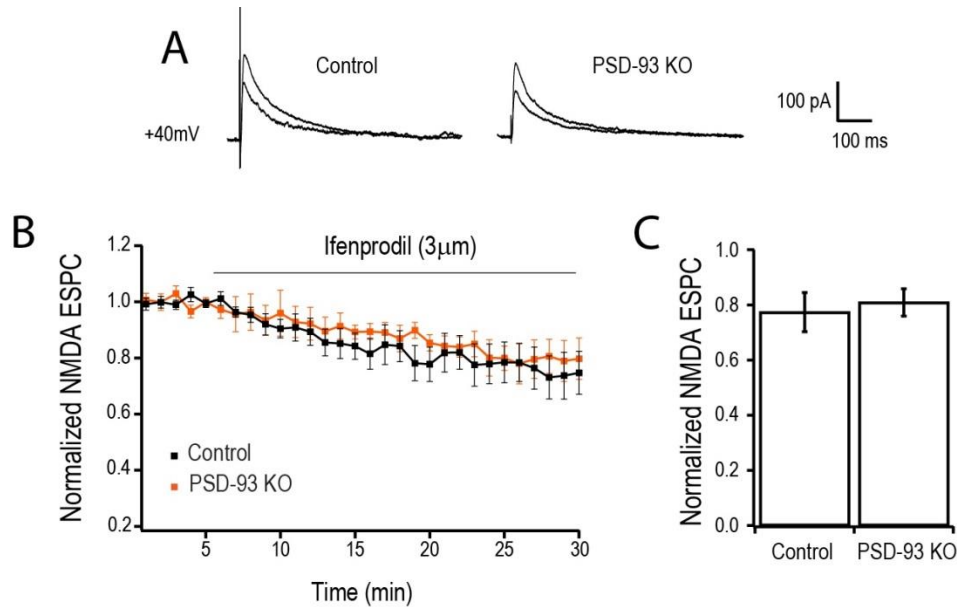
Figure 3. 3: Normal GluN2B contribution to NMDAR EPSCs in the absence of PSD-93.

A: Representative Control and PSD-93 KO NMDAR EPSCs before and 25 min after GluN2B blockade by Ifenprodil 3μM. AMPARs and inhibition were continuously blocked by NBQX 5μM and picrotoxin 50μM, respectively. **B**: Time course of GluN2B blocking by Ifenprodil wash-in. **C**: Bar graphs showing NMDAR EPSC amplitude 15-25 min after Ifenprodil 3μM normalized to the initial NMDAR EPSC amplitude. The fractional block is not affected by PSD-93 deletion (Control vs. PSD-93, $p>0.05$ t-test). Data presented as mean ± SEM.

The results suggest that PSD-93 does not modulate basal NMDAR neurotransmission in L4-L2/3 synapses at PD21-30. The reduced NMDAR cell-surface expression reported by other groups might represent an age-dependent or selective modulation of extra synaptic NMDARs by PSD-93. The increased AMPA/NMDA ratio in PSD-93 KO might be the result of increased postsynaptic AMPAR function in L2/3 neurons.

3.3 Increased AMPAR mEPSC frequency, but normal mEPSC amplitude, in the absence of PSD-93.

To further dissect the possible role of PSD-93 governing AMPAR neurotransmission, spontaneous AMPAR miniature EPSCs (mEPSCs) were recorded in 1μM TTX to block action potential evoked EPSCs. Each mEPSC is the response of

single synapses to a single spontaneously released vesicle (Fatt and Katz, 1952; Burgard and Hablitz, 1993).

mEPSC amplitude is defined as quantal size: the postsynaptic response of single synapses to the release of single vesicles. mEPSC frequency represents the number of synapses activated in a given time interval. It is the combined result of release probability (*Pr*) and number of AMPAR-containing synapses.

Pr is directly correlated with mEPSC frequency; in high *Pr* mEPSC frequency tends to be higher and in low *Pr* lower. Alternatively, high number of AMPAR-containing synapses can lead to higher mEPSC frequency and low number of AMPAR-containing synapses to lower mEPSC frequency.

Increased mEPSC frequency (represented as reduced average inter-event interval) was detected in the absence of PSD-93 (Fig. 3.4; Control, 0.28s ± 0.03 [n/m = 17/3]; PSD-93 KO, 0.19s ± 0.01 [n/m = 17/3]; $p < 0.05$, Kolmogorov-Smirnov test). In contrast, mEPSC amplitude was not influenced (Fig 3.5; Control 14.67 pA ± 0.67 [n/m = 17/3]; PSD-93 KO, 14.02 pA ± 0.30 [n/m = 17/3]; p = 0.95; Kolmogorov-Smirnov test), excluding a role of PSD-93 in regulating quantal size.

As commented earlier, changes in mEPSC frequency can be interpreted as changes in Pr or number of AMPAR-containing synapses. Therefore, both hypotheses were tested with electrophysiological approaches (for Pr see section 3.4; for AMPAR-containing synapses see section 3.8).
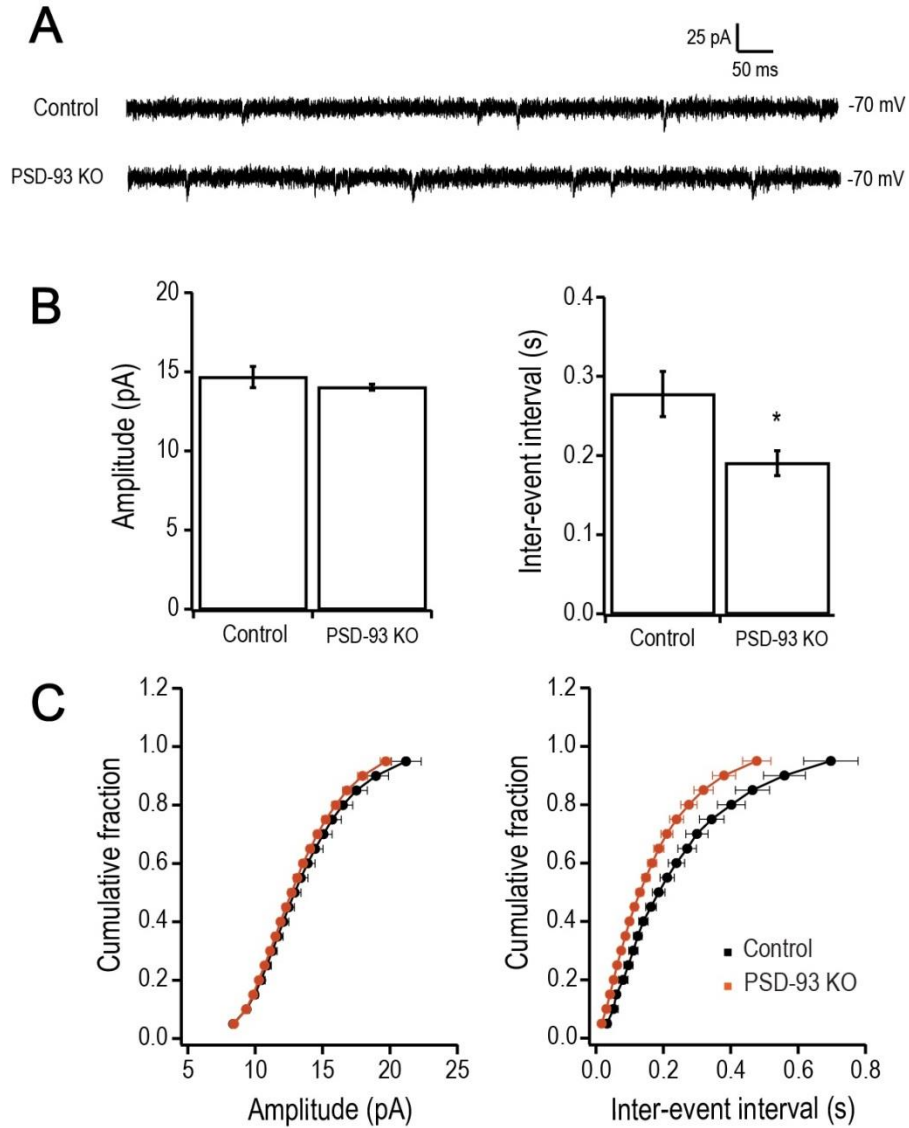
Figure 3. 4: Increased AMPAR neurotransmission in the absence of PSD-93.

A: sample traces of mEPSCs recorded from Control and PSD-93 KO slices. Action potentials were blocked by TTX 1μM and inhibition blocked by picrotoxin 50μM. **B:** Summary bar graphs showing increased mEPSC frequency (reduced inter event interval), but normal mEPSC amplitude, in PSD-93 KO. **C:** Cumulative distribution of the data. For each neuron, 400 mEPSCs were recorded. Data presented as mean ± SEM.

3.4 Normal release probability in the absence of PSD-93.

3.4.1 Analysis of release probability with paired pulse ratio experiments.

To unequivocally determine whether the increased AMPAR neurotransmission in PSD-93 KO was influenced by changes in release probability (*Pr*), Paired-Pulse Ratio (PPR) of AMPAR EPSCs was measured. PPR is a form of short-term plasticity classically thought to be inversely correlated with *Pr* at glutamatergic synapses (Dobrunz and Stevens, 1997; Zucker and Regehr, 2002). Pairs of AMPAR EPSCs were evoked with inter-stimulus intervals of 50 ms and 100 ms, PPR was the ratio of second to first EPSC peak amplitude.

Paired pulse facilitation is observed when the second AMPAR EPSC is higher than the first. When an action potential reaches the presynaptic terminal, membrane depolarization activates voltage-gated calcium channels, which mediate calcium influx required for vesicle fusion and neurotransmitter release. In low *Pr* many vesicles are not released after an action potential and stay docked to the pre-synaptic membrane. If an additional action potential follows shortly after, residual calcium from the first action potential, which has not been totally cleared, will build up with calcium from the second action potential. The resulting increase in calcium leads to greater vesicle fusion and, therefore, higher postsynaptic response.

Paired pulse depression is observed when the second AMPAR EPSC is lower than the first. In high *Pr* many vesicles are released when the terminal is depolarized by an action potential, depleting the readily-releasable pool. In this scenario, fewer vesicles will be left for a second action potential, and the magnitude of vesicle fusion will be lower even in the presence of increased calcium.

Therefore, synapses with low initial *Pr* are likely to exhibit facilitation, and synapses with high initial *Pr* are likely to exhibit depression. In the present work, both Control and PSD-93 KO synapses showed paired pulse facilitation and were not different (Fig 3.5; Control, 1.20 ± 0.07 at 50ms, 1.05 ± 0.04 at 100ms, [n/m = 10/3]; PSD-93 KO, 1.15 ± 0.09 at 50ms, 1.06 ± 0.07 at 100ms, [n/m = 10/5]; Control vs. PSD-93 KO, $p = 0.66$ at 50ms and $p = 0.50$ at 100ms, t-test). The results suggest normal *Pr* in the absence of PSD-93.
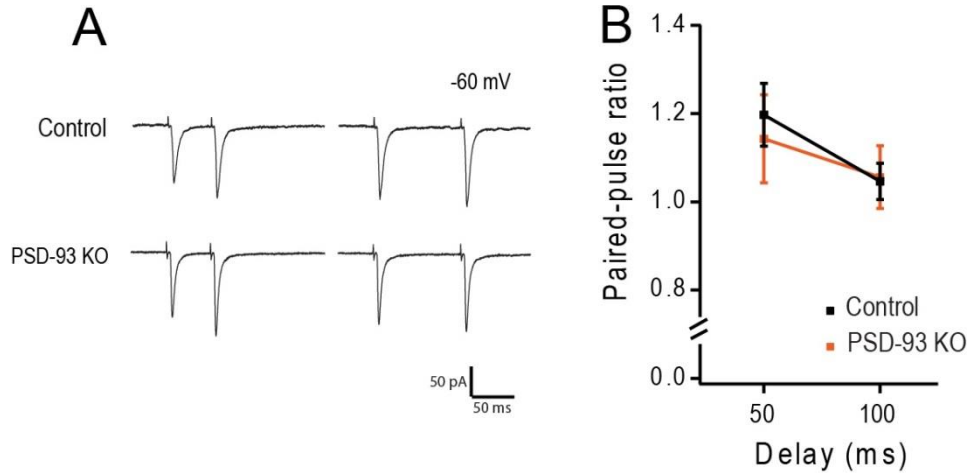
Figure 3. 5: Normal Paired pulse ratio in the absence of PSD-93.

A Average traces showing paired AMPAR EPSCs (50 and 100 ms apart), for both Control and PSD-93 KO slices. **B** The modest paired pulse facilitation is not affected by PSD-93 deletion (Control vs. PSD-93 KO, $p>0.05$ at 50ms and 100ms, t-test). Data presented as mean ± SEM.

3.4.2 Analysis of release probability with MK-801.

Despite its common use to evaluate *Pr*, PPR can be potentially affected by postsynaptic AMPAR desensitization (Heine et al, 2008) and by changes in presynaptic calcium channels during repetitive stimulation (Xu et al, 2007). Therefore, *Pr* was measured more directly using a standard assay: the rate of blockade of NMDAR EPSCs by MK-801, an irreversible open-channel blocker (Hessler et al, 1993, Rosenmund et al, 1993). This approach is AMPAR-independent and does not involve repetitive stimulations that cause changes in presynaptic calcium channels. Furthermore, it is suitable to the present study as NMDARs were not affected by PSD-93 deletion.

In the presence of MK-801, presynaptic stimulation leads to NMDAR blockade only at synapses which release a vesicle. MK-801 is an irreversible blocker, therefore continuous stimulation leads to a progressive decay in NMDAR EPSC amplitude. In high *Pr*, more vesicles are released following presynaptic stimulation; more NMDARs are activated and blocked leading to faster decay of NMDAR EPSCs. In low *Pr*, fewer vesicles are released following presynaptic stimulation, less NMDARs are activated and blocked leading to slower decay of NMDAR EPSCs. Therefore, the time constant of NMDAR EPSC decay is inversely related to *Pr*.

The progressive blockade of NMDAR by MK-801 5μM was not affected by PSD-93 deletion (Fig. 3.6), consistent with results from PPR experiments. Single exponential fit showed no difference in decay constant between Control and PSD-93 KO (Control $\tau = 10.51 \pm 0.94$ [n/m = 10/3]; PSD-93 KO, $\tau = 10.52 \pm 1.42$ [n/m = 11/3]; p>0.05).

The results suggest that *Pr* is not affected by PSD-93 deletion. Therefore, changes in *Pr* are unlikely to influence AMPAR neurotransmission in PSD-93 KO slices, reinforcing a specific postsynaptic role of PSD-93.
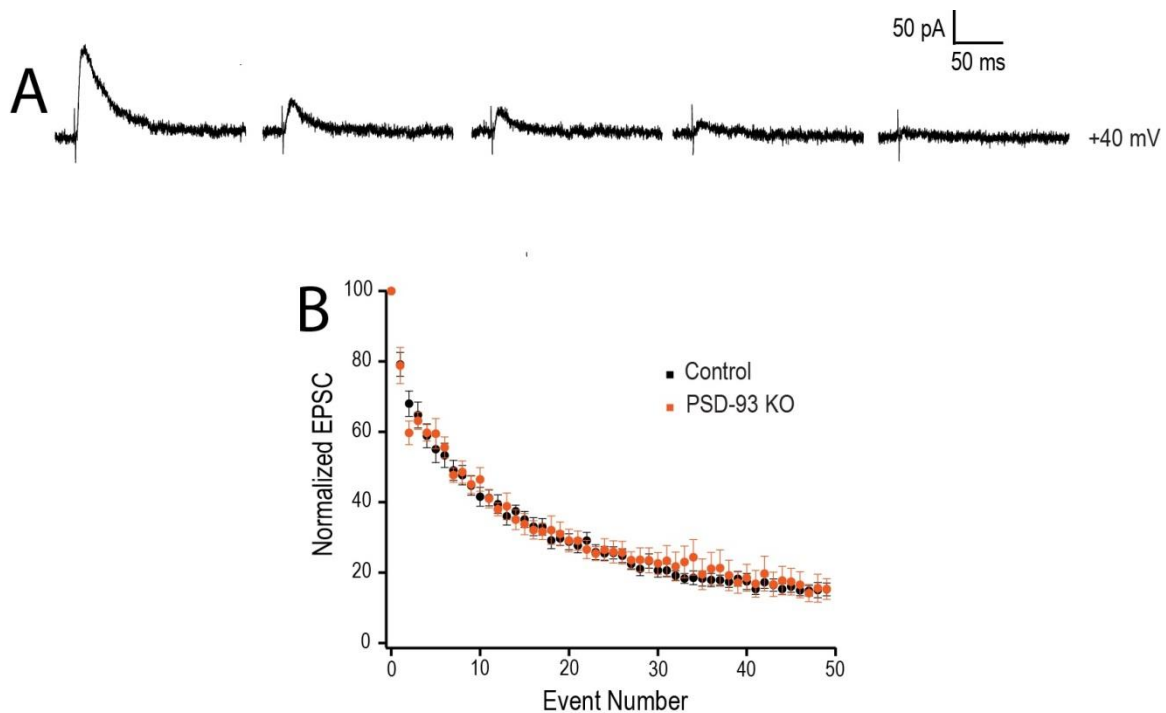
Figure 3. 6: PSD-93 deletion does not affect NMDAR EPSC decay in the presence of MK-801.

A: sample NMDAR EPSCs from a control slice recorded at the 1st, 10th, 20th, 30th, and 40th consecutive presynaptic stimulation, respectively. Note the progressive decay of synaptic responses in the presence of MK-801 5μM. AMPARs were blocked by NBQX 5μM and inhibition by picrotoxin 50μM. **B:** Summary graph showing no change in NMDAR EPSC decay in the absence of PSD-93. Data presented as mean ± SEM.

3.5   Normal quantal size at L4-L2/3 synapses in the absence of PSD-93.

Analyses of spontaneous mEPSCs are widely used to evaluate the integrity of glutamatergic neurotransmission in brain slices. However, mEPSCs lack specificity, as they can originate from any synaptic connection into the recorded neuron.

To record quantal responses specifically at L4-L2/3 synapses, voltage-clamp experiments were performed in a modified aCSF containing strontium 8mM and no calcium. In the presence of calcium, action potentials cause synchronous release of synaptic vesicles by presynaptic terminals. When calcium is replaced with strontium synchronous release is suppressed. In this scenario, presynaptic stimulation leads to a prolonged asynchronous release of synaptic vesicles (Fig 3.7A).
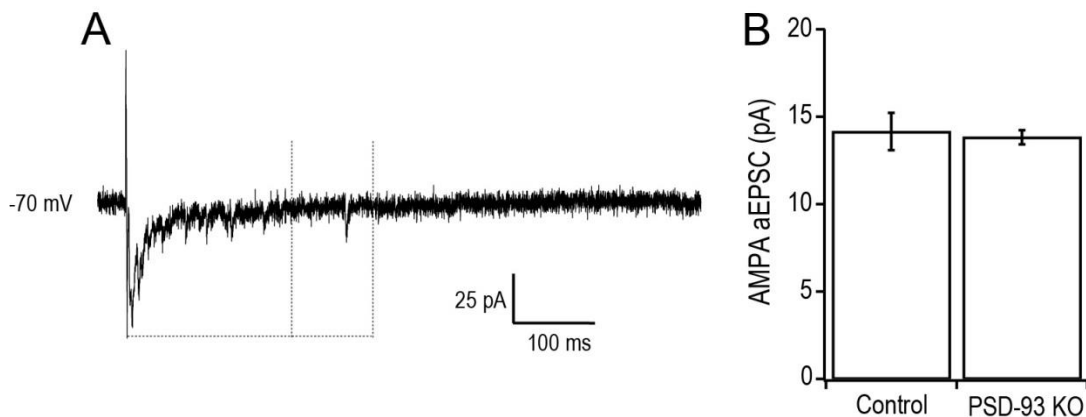
Figure 3. 7: Normal quantal size at L4-L2/3 synapses in the absence of PSD-93.

A: Representative trace of an aEPSC experiment, vertical dashed lines define the time window in which aEPSCs were measured (200-300 ms after presynaptic stimulation). At least 50 aEPSCs were recorded per neuron. Extracellular calcium was replaced with strontium 8mM and inhibition blocked by picrotoxin 50 mM. **B:** Summary bar graphs showing no effect of PSD-93 deletion on aEPSC amplitude (Control vs. PSD-93 KO, p>0.05, t-test). Data presented as mean ± SEM.

In strontium, EPSCs evoked by presynaptic stimulation are characterized as discrete asynchronous mEPSC-like responses (aEPSCs). Each aEPSC is the response to a single synaptic vesicle released from the stimulated presynaptic afferent. Thus, the quantal size of AMPARs, specifically at L4-L2/3 synapses, can be measured in relative isolation from other synaptic inputs.

aEPSCs were identical in Control and PSD-93 KO slices (Fig. 3.7; Control, 14.15 pA $\pm$ 1.07 [n/m = 6/2]; PSD-93 KO, 13.84 $\pm$ 0.40 [n/m = 8/2]; p = 0.94, t-test). Therefore, in agreement with mEPSC experiments, PSD-93 deletion does not alter quantal size at L4-L2/3 synapses.

3.6 Normal AMPAR current-voltage relationship in the absence of PSD-93.

To further analyze the role of PSD-93 in regulating AMPAR neurotransmission, a rectification index experiment was used to evaluate AMPAR subunit composition in PSD-93 KO slices.

AMPARs are tetramers of the subunits GluA1-GluA4. The different subunits bind to distinct interacting partners, differentially modulate AMPAR trafficking and control the ionic conductance of single-channels (Malinow and Malenka, 2002; Bredt and Nicoll, 2003). GluA2 subunits render AMPARs calcium impermeable. In contrast, GluA2-lacking AMPARs are permeable to calcium and pass less current at positive potentials. As a consequence of these biophysical differences, GluA2-containing AMPARs present linear current-voltage relationship. GluA2-lacking AMPARs present inward rectification (reduced current at positive potentials) due to voltage-dependent block by intracellular polyamines. Thus, GluA2-containing AMPAR EPSCs at positive membrane potentials are higher than GluA2-lacking AMPAR EPSCs. Consequently, rectification index (AMPAR EPSCs at -70mV normalized to AMPAR EPSCs at +50mV) is lower for GluA2-containing AMPARs.

The AMPAR rectification index was not affected by PSD-93 deletion (Fig. 3.8; Control, 2.13 $\pm$ 0.29 [n/m = 7/2]; PSD-93 KO, 2.04 $\pm$ 0.25 [n/m = 5/2]; p = 0.82, t-test), suggesting no major role for PSD-93 in regulating AMPAR subunit composition in cortical synapses.
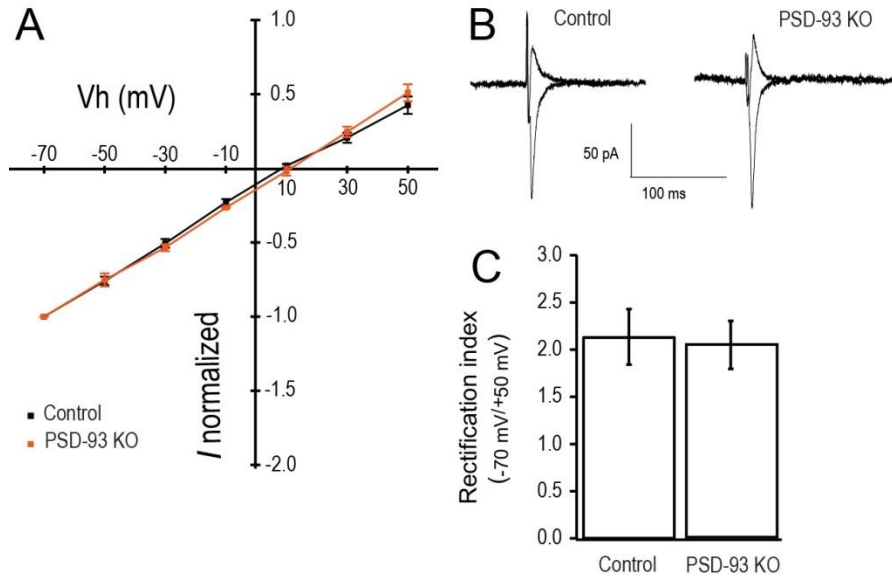
Figure 3. 8: Normal AMPAR rectification index in the absence of PSD-93.

A: Summary graph showing current -voltage (*I* - Vh) relationship of isolated AMPAR EPSCs from Control and PSD-93 KO slices. NMDARs were blocked by APV 50μM, inhibition blocked by picrotoxin 50μM and internal solution supplemented with spermine 100μM. **B**: Samples traces of AMPAR EPSCs recorded at -70 mV (inward current) and +50 mV (outward current) from Control and PSD-93 KO slices. **C**: rectification index is AMPAR amplitude at -70 mV normalized to AMPAR amplitude at +50 mV. Summary bar graphs showing normal rectification index in the absence of PSD-93 (Control vs. PSD-93 KO, $p>0.05$, t-test). Data presented as mean ± SEM.

3.7 Increased AMPAR unitary EPSCs in the absence of PSD-93.

In order to directly measure the strength of AMPAR neurotransmission at L4-L2/3 connections, unitary AMPAR responses (uEPSCs) were recorded. A bipolar stimulating electrode was placed in L4 and L2/3 neurons were voltage-clamped at -70 mV. In each recording, stimulation intensity was slowly increased until the smallest evoked EPSC, here defined as uEPSC, could be identified. Once this condition was obtained, 50 sweeps were recorded at 0.17Hz. The weak presynaptic stimulation leads to a combination of postsynaptic responses (uEPSCs) and failures. Presumably, uEPSCs are putative single axon evoked EPSCs from axons in L4 to L2/3 pyramidal neurons. The monosynaptic nature of these responses is evidenced by the short and constant delay between presynaptic stimulation and uEPSC peak amplitude, at the range of 5-7 ms (fig 3.9A).
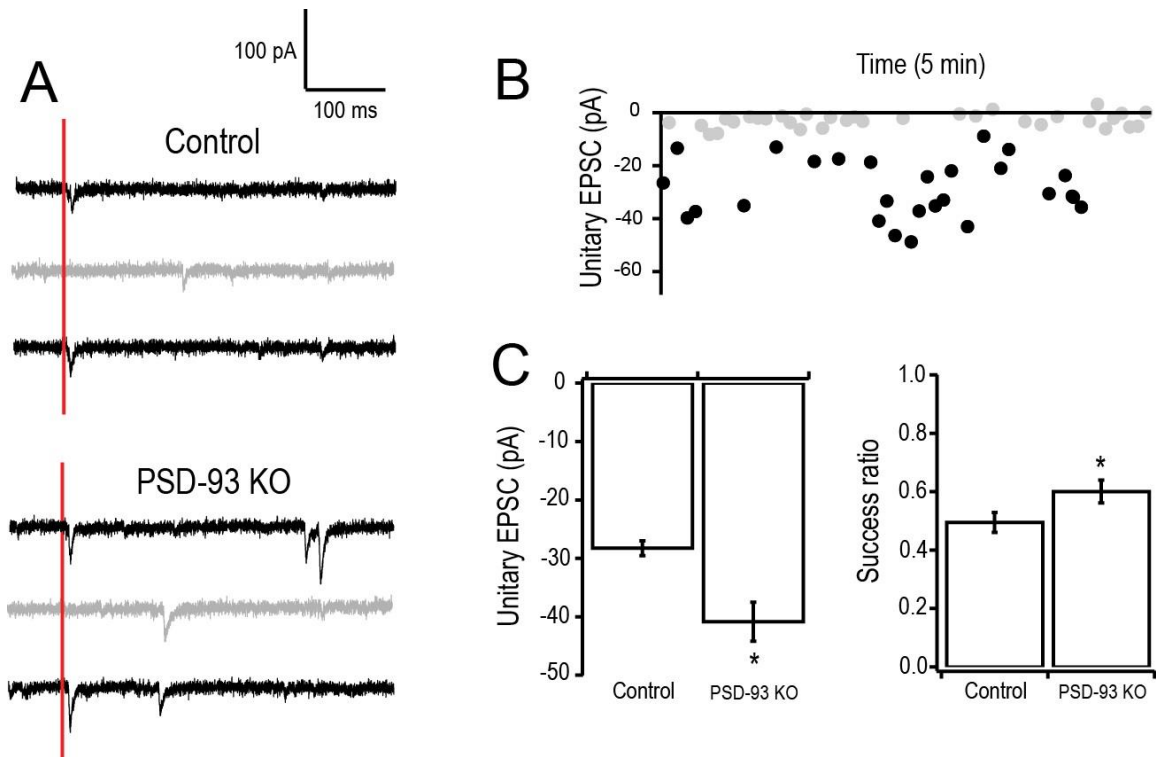
Figure 3. 9 Increased AMPAR uEPSC in the absence of PSD-93.

A: sample consecutive traces of AMPAR uEPSCs (black) and synaptic failures (gray) in Control and PSD-93 KO slices. Extracellular stimulation was applied as indicated in red. AMPAR uEPSCs peaks were within 5 to 8 ms after stimulation. Recording was at -70 mV and inhibition blocked by picrotoxin 50μM. **B:** Analysis of AMPAR uEPSCs (black) and synaptic failures (gray) in a Control slice. **C:** Summary bar graphs showing increased AMPAR eEPSC (Control vs. PSD-93 KO, p<0.05, t-test), and increased success ratio (Control vs. PSD-93 KO, p<0.05, t -test) in PSD-93 KO slices. Data presented as mean ± SEM.

Consistent with the increased AMPA/NMDA ratio and no change in NMDAR uEPSCs, PSD-93 KO slices presented increased AMPAR uEPSC amplitude (Fig 3.9; Control, 28.27 pA ± 1.27 [n/m = 19/4]; PSD-93 KO, 40.85 pA ± 3.33 [n/m = 21/4]; p<0.05, t-test). As mentioned, in uEPSC recordings a fraction of presynaptic stimulations fail to elicit detectable EPSCs. The success ratio was defined as number of detected uEPSCs divided by total number of presynaptic stimulations. In uEPSC experiments, a modest increase of success ratio was observed in PSD-93 KO when compared to Control slices (Fig. 3.9; Control, 0.49 ± 0.03 [n/m = 19/4]; PSD-93 KO, 0.60 ± 0.04 [n/m = 21/4]; p<0.05; t-test).

The present data supports the notion that postsynaptic changes at L4-L2/3 connections characterize the increased AMPAR neurotransmission in PSD-93 KO at PD-21-30. This postsynaptic change is not caused by modifications is the number or conductance of AMPAR at existing synapses. Thus, PSD-93 deletion might cause an increase in the number of AMPAR-containing synapses in L4-L2/3 connections.

3.8 Silent synapses in visual cortex.

In the brain, some synapses contain functional postsynaptic NMDARs but not AMPARs. At resting membrane potential, neurotransmitter release fails to elicit EPSCs in these synapses and for this reason they are considered to be silent (Isaac et al, 1995; Liao et al, 1995). These AMPAR-lacking silent synapses are suggested to be immature synapses; their relative number tends to decrease as AMPARs are gradually added to postsynaptic sites during normal brain development (Rumpel et al, 1998).

In order to evaluate whether silent synapses could be detected in L4-L2/3 connections of mouse visual cortex, a failure analysis of minimal EPSCs was performed in slices from mice at PD3-5, PD10-12 just before eye-opening and PD21-30 at the critical period for cortical plasticity. L2/3 pyramidal neurons were voltage-clamped and minimal EPSCs were obtained by adjusting extracellular stimulation to evoke postsynaptic responses and failures at L4-L2/3 synapses (Fig 3.10A-B). Percentage of silent synapses was estimated by comparing the failure rate at -60 mV and +40mV (Liao et al, 1995; Huang et al 2009).

The percentage of silent synapses gradually decreased during normal development of L4-L2/3 connections (Fig. 3.10C; Control PD3-5, 80.0% ± 5.2 [n/m = 13/3]; Control PD10-12, 58.6% ± 4.3 [n/m = 13/3]; Control PD21-30, 23.8% ± 5.7 [n/m = 18/6]), in agreement with the general assumption that they turn into mature transmitting synapses during development (Rumpel et al, 1998).
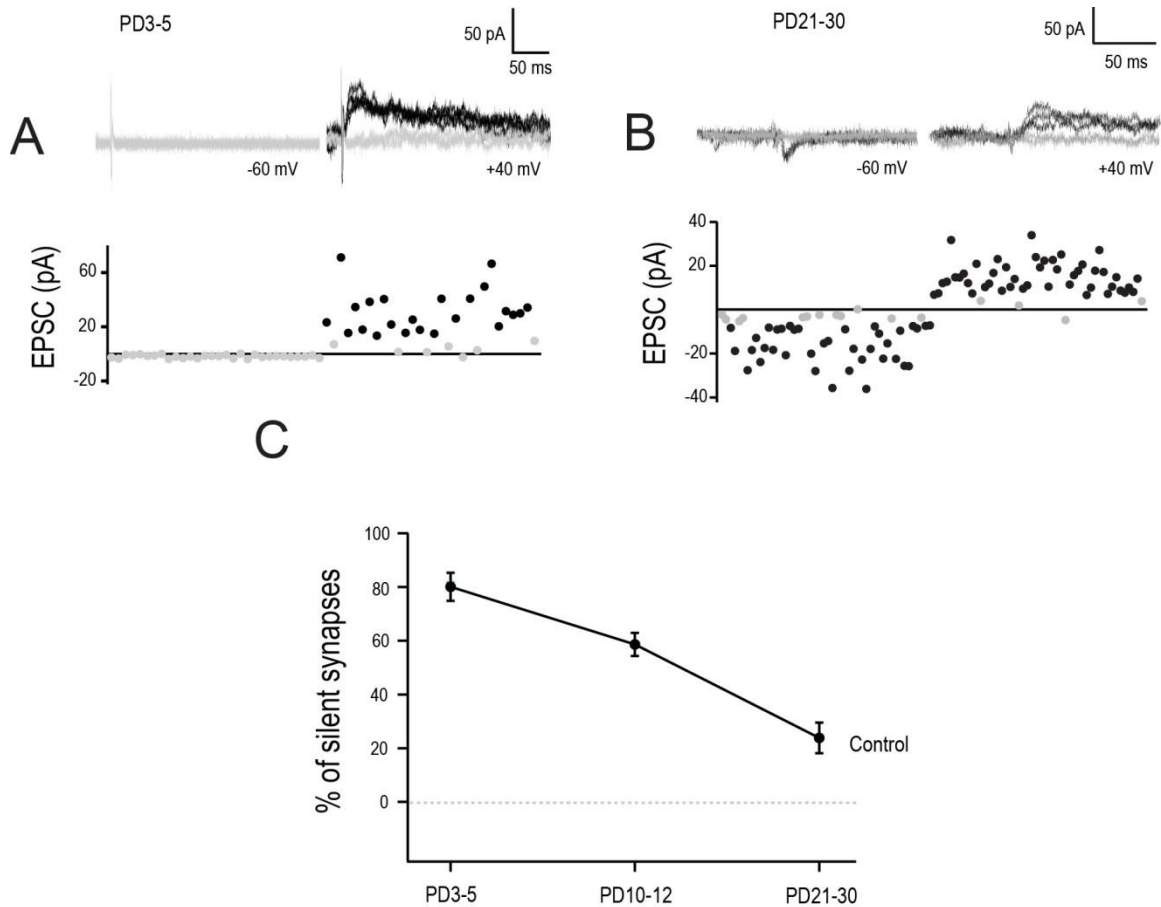
Figure 3. 10: Silent synapses in visual cortex.

A-B: sample traces of minimal EPSCs recorded at -60mV and +40 mV in two different ages (at PD3-5 [A] and PD21-30 [B]). Corresponding EPSC analysis is under the sample traces (synaptic responses are black and failures gray). Traces in A show no synaptic response at -60 mV; therefore in this experiment 100% synapses were silent. **C:** Percentage of silent synapses at different ages (Control PD3-5 vs. Control PD10-12, p<0.05; Control PD10-12 vs. Control PD21-30, p<0.05; Control PD3-5 vs. Control PD21-30, p<0.05, t-test with Bonferroni correction). Inhibition was continuously blocked by picrotoxin 50μM. Data presented as mean ± SEM.

3.9 PSD-93 and PSD-95 present opposite roles in synaptic maturation.

In order to analyze whether PSD-93 increases AMPAR neurotransmission by changing the fraction of silent synapses, failure analysis of minimal EPSCs was additionally performed in PSD-93 KO slices.

Silent synapses were not affected by PSD-93 deletion at PD3-5 (Fig 3.11; Control PD3-5, 80.0% ± 5.2 [n/m = 13/3]; PSD-93 KO PD3-5 85.3% ± 3.7 [n/m = 11/4]; p=0.44,

t-test). However, when compared to Control, PSD-93 deletion reduced the percentage of silent synapses both at PD10-12 and PD21-30. (Fig. 3.11; Control PD10-12, 58.6% ± 4.3 [n/m = 13/3]; PSD-93 KO PD10-12, 30.5% ± 6.1 [n/m = 22/5]; p<0.05, t–test. Control PD21-30, 23.8% ± 5.7 [n/m = 18/6]; PSD-93 KO PD21-30, 1.0% ± 6.4 [n/m = 12/6]; p<0.05, t-test). Thus, PSD-93-lacking synapses appear to present accelerated synaptic maturation. In addition, unaffected silent synapses at PD3-5 is consistent with the absence of PSD-93 in this developmental stage (Sans et al, 2000)

Previous work on hippocampus suggested that PSD-93 and PSD-95 appear to have redundant roles on basal glutamateric neurotransmission (Elias et al, 2006). However, PSD-95 deletion is strongly related to reductions in AMPAR neurotransmission and, in the present work, PSD-93 deletion had the opposite effect, increasing AMPAR neurotransmission. Thus, in order to better clarify this scenario, silent synapses were measured in PSD-95 KO mice, at PD10-12 and PD21-20.

PSD-95 KO and Control slices exhibited similar percentage of silent synapses at PD10-12 (Fig. 3.11; Control PD10-12, 58.6% ± 4.3 [n/m = 13/3]; PSD-95 KO PD10-12, 55.3% ± 3.2 [n/m = 10/3]; p=0.57, t-test). However, the percentage of silent synapses remained high in PSD-95 KO at PD21-30 (Fig. 3.11; Control PD21-30, 23.8% ± 5.7 [n/m = 18/6]; PSD-95 KO PD21-30, 48.1% ± 5.1 [n/m = 8/3]; p<0.05, t-test). This suggests that normal synaptic maturation failed to occur in PSD-95 KO after PD10-12, as about 50% of synapses remained silent at PD21-30.

The results suggest that PSD-93 and PSD-95 might play opposite roles governing silent synapses in visual cortex. PSD-93 deletion caused accelerated synaptic maturation, characterized by reduced fraction of silent synapses at PD10-12 and PD21-30. In contrast, PSD-95 deletion resulted in reduced synaptic maturation and increased fraction of silent synapses when compared to Control at PD21-30. These opposite roles were unexpected; therefore, to better clarify this scenario, silent synapses were additionally measured in the absence of both PSD-93 and PSD-95.
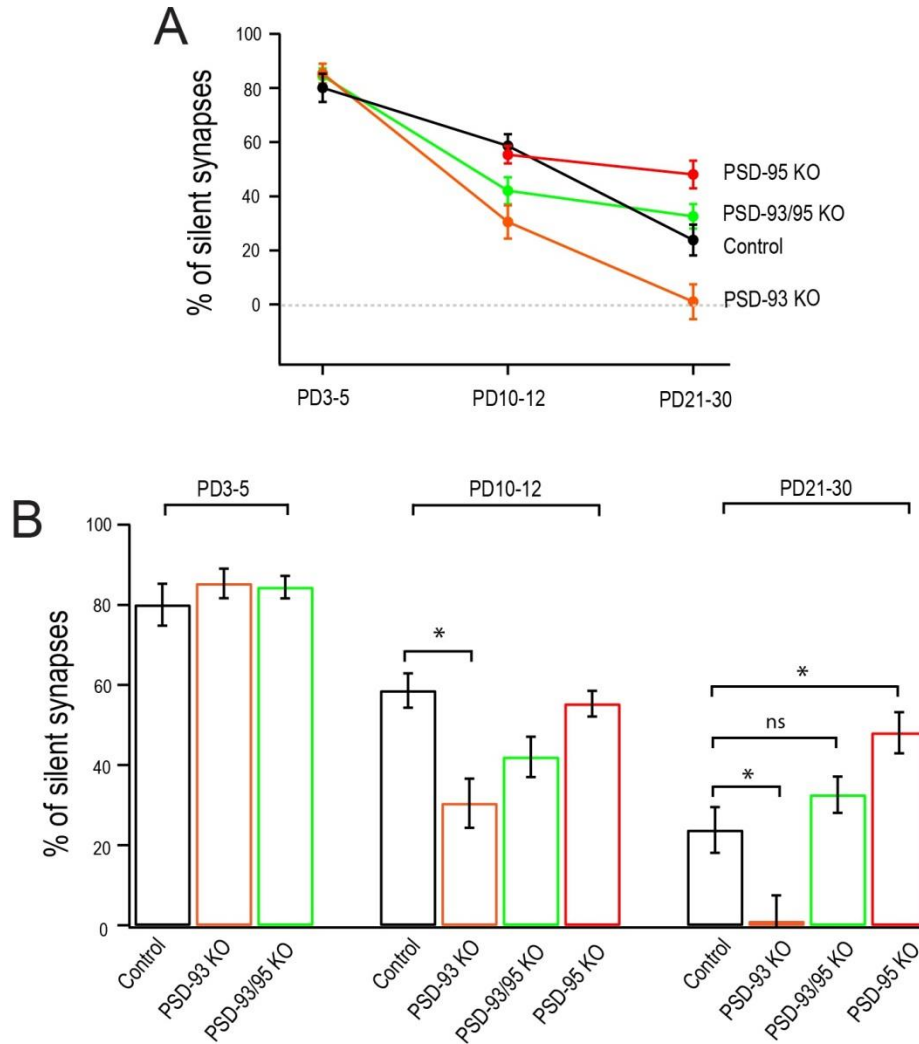
Figure 3. 11: PSD-93 and PSD-95 have opposite roles in synaptic maturation.

A: PSD-93 and PSD-95 play opposite roles in regulating maturation of silent synapses. (Control PD10-12 vs. PSD-93 KO PD10-12, $p<0.05$; Control PD21-30 vs. PSD-93 KO PD21-30, $p<0.05$; Control PD21-30 vs. PSD-95 KO PD21-30, $p<0.05$, t-test with Bonferroni correction). Data presented as mean ± SEM. PSD-95 KO data was obtained by Xiaojie Huang. PSD-93/95 KO data was obtained by Xiaojie Huang and Plinio Favaro.

Effective deletion of PSD-93 and PSD-95 was obtained with two different approaches. First, silent synapses were recorded in slices from PSD-93/95 double KO mice at PD3-5 (n/m =5/1), PD10-12 (n/m = 5/1) and PD21-30 (m/n = 13/3). A second approach involved viral-mediated knock-down of endogenous PSD-95 in PSD-93 KO mice. A viral vector containing shRNA against PSD-95 was injected into the visual

cortex of PSD-93 KO newborn mice. shRNA expression was coupled to GFP, therefore infected neurons lacking both PSD-93 and PSD-95 presented fluorescence and were visually identified in acute brain slices at PD10-12 (n/m = 23/4) and PD21-30 (n/m = 16/4). Results obtained with the two different approaches were similar and therefore combined.

Similarly to PSD-93 KO, there was a tendency towards reduction of silent synapses in PSD-93/95 KO when compared to Control at PD10-12 (Fig. 3.11; Control PD10-12, 58.6% ± 4.3 [n/m = 13/3]; PSD-93/95 KO PD10-12, 42.0% ± 5.0 [n/m = 28/6]; p=0.043, t-test), however the difference was rejected by posthoc Bonferroni correction. At PD21-30, PSD-93 KOs have less silent synapses and PSD-95 KOs more silent synapses. In contrast, PSD-93/95 double KOs remained indistinguishable from Control (Fig. 3.11; Control PD21-30, 23.8% ± 5.7 [n/m = 18/6]; PSD-93/95 KO PD21-30, 32.6% ± 4.6 [n/m = 29/7]; p=0.31, t-test).

Results obtained with PSD-93/95 double KO support the unexpected idea that PSD-93 and PSD-95 play opposite roles governing maturation of cortical synapses. The increased percentage of silent synapses in the absence of PSD-95 is consistent with previous works, in which the strength of AMPAR neurotransmission and the relative number of silent synapses are modulated by bidirectional changes in PSD-95 levels (Stein et al, 2003; Beique and Andrade, 2003; Beique et al, 2006).

Concerning PSD-93, less information was available. The present data supports the notion that accelerated synaptic maturation, evidenced by precocious unsilencing of silent synapses at L4-L2/3 connections, leads to increased AMPAR neurotransmission in PSD-93 KO at PD-21-30. Furthermore, a novel and unexpected scenario appears to emerge, with PSD-93 presenting an opposite role, when compared to PSD-95, on basal glutamatergic neurotransmission.

3.10 Normal membrane properties in the absence of PSD-93.

PSD-93 KO synapses presented increased AMPAR neurotransmission. In juvenile rodents, changes in strength of excitatory synapses can trigger homeostatic changes in excitability of cortical pyramidal neurons (Maffei and Turrigiano, 2008). Additionally, PSD-93 is known to interact with Kv4.2, an A-type K^+ channel widely expressed in soma,

dendrites and spines of inhibitory and excitatory cortical neurons (Kim and Sheng, 2004; Burkhalter et al, 2006). Kv4.2 channels are suggested to play specific roles in the generation of action potentials and regulation of repetitive firing. Indeed, increased cell-surface expression of Kv4.2 leads to reduced neuronal excitability in hippocampus (Varga et al, 2004). Thus, PSD-93 can potentially affect neuronal excitability directly, by interacting with Kv4.2 channels; and indirectly, by modulating excitatory synaptic transmission and eliciting compensatory changes in intrinsic excitability.

To probe PSD-93 roles in neuronal excitability, whole-cell current-clamp electrophysiology was used. Resting membrane potential and input resistance were measured just after obtaining the current-clamp configuration. Intrinsic excitability was assessed by measuring the number of action potentials triggered by different levels of depolarizing currents (Fig. 3.12).
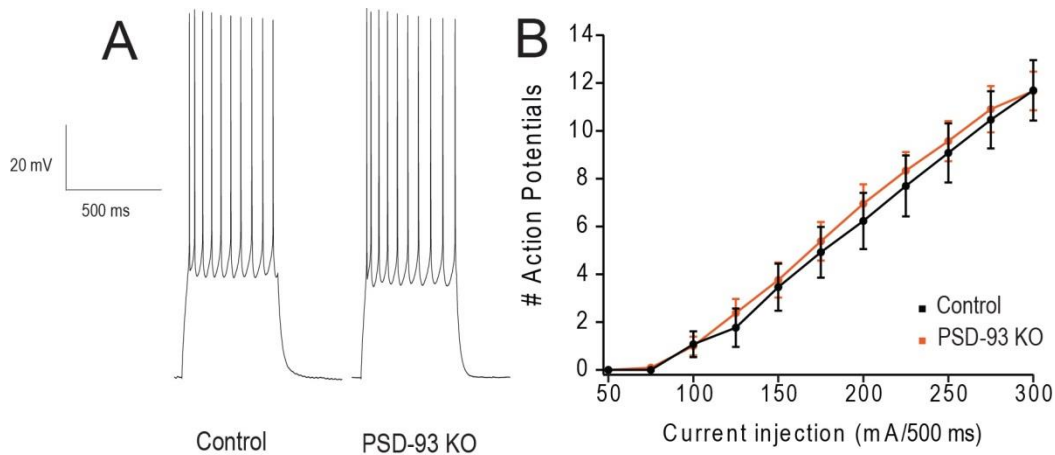
Figure 3. 12: Normal intrinsic excitability in the absence of PSD-93.

A: Example firing in response to depolarizing current (250mA/500ms) for a Control and a PSD-93 KO pyramidal neuron. AMPARs and NMDARs were blocked by NBQX 5μM and APV 50μM, respectively. Inhibition was not blocked as it causes unstable current-clamp recordings. **B**: Number of actions potentials versus current intensities for Control and PSD-93 KO, showing no influence of PSD-93 deletion on induced cell-firing. (Control vs. PSD-93 KO, $p>0.05$ for all current intensities, t-test). Data presented as mean ± SEM.

PSD-93 deletion had no effect on resting membrane potential (Control, -74.85mV ± 1.60 [n/m = 13/2]; PSD-93 KO, -75.14mV ± 1.22 [n/m = 22/2]; p=0.93, t-test), input resistance (Control, 103.61MOhm ± 8.15 [n/m = 13/2]; PSD-93 KO, 116.76MOhm ± 7.16 [n/m = 22/2]; p=0.24, t-test), or intrinsic excitability (Fig 3.12).

3.11 Normal GABA/AMPA ratio in the absence of PSD-93.

Inhibitory GABAergic interneurons are key elements regulating the activity of local cortical circuits. As an example, by reducing the relative levels of intracortical inhibition it is possible to promote plasticity within the visual cortex (Sales et al, 2007; Greifzu et al, 2014). Glutamatergic input is a crucial factor determining the activity of inhibitory interneurons, which are known to express not only PSD-93, but also PSD-95 and SAP-97 (Akgul et al, 2010).

GABAergic inhibitory postsynaptic currents (GABA$_A$ IPSCs) were reliably evoked on L2/3 pyramidal neurons by extracellular stimulation delivered to L4. Isolated GABA$_A$ IPSCs were recorded at +5mV (reversal potential for AMPARs), and AMPAR EPSCs were recorded at -70 mV (reversal potential for GABA$_A$). NMDARs were continuously blocked by APV 50μM. GABA/AMPA ratio is defined as GABA$_A$ IPSC amplitude normalized to AMPAR EPSC amplitude.

Electrical stimulation at L4 evokes GABAA IPSCs at L2/3 neurons via two different mechanisms: 1) monosynaptically, by direct stimulation of GABAergic axons; and 2) bisynaptically, by stimulating glutamate release on GABAergic interneurons, inducing consequent firing and GABA release at the L2/3 target neuron.

In the present recording configuration it is estimated that, on average, 70% of GABAR IPSCs are blocked by AMPAR antagonist NBQX, suggesting most of GABA$_A$ IPSCs to be evoked bisynaptically (Huang, 2014). Therefore, GABA$_A$ IPSCs recorded at L2/3 pyramidal neurons strongly relies on the integrity of AMPAR neurotransmission at inhibitory interneurons.

PSD-93 deletion caused increased AMPAR neurotransmission in L4-L2/3 synapses at PD21-30. In case PSD-93 has a specific role in those synapses, but not in excitatory inputs to inhibitory interneurons, a decrease in GABA/AMPA ratio would be expected.

However, the GABA/AMPA ratio was not affected by PSD-93 deletion (Fig. 3.13; Control, 2.07 ± 0.17 [n/m = 18/3]; PSD-93 KO, 2.20 ± 0.18 [n/m = 22/3]; p = 0.60 t-test).
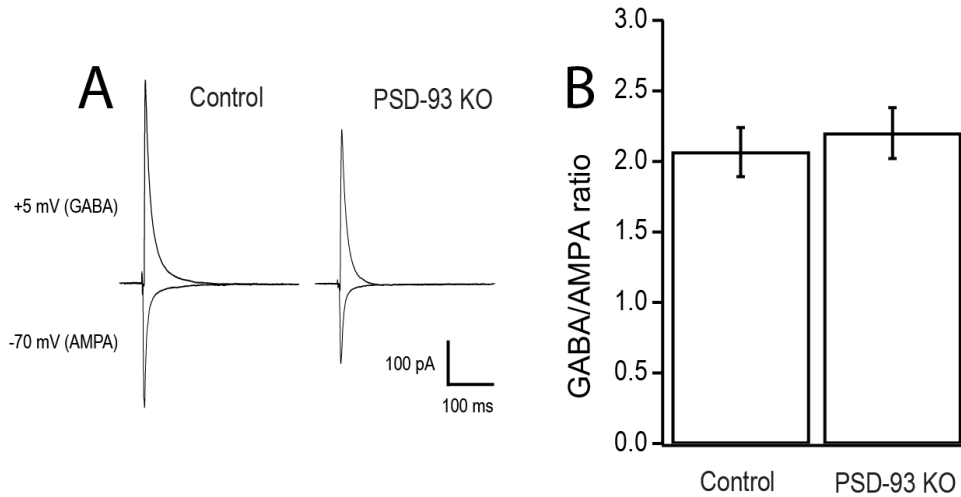
Figure 3. 13: Normal GABA/AMPA ratio in the absence of PSD-93.

A: representative average AMPAR EPSCs recorded at -70mV (reversal potential of GABAR), and average GABAR IPSCs recorded at +5mV (reversal potential of AMPAR). NMDARs were blocked by APV 50μM. **B**: Summary bar graph showing normal GABA/AMPA ratio in the absence of PSD-93 (Control vs. PSD-93 KO, p>0.05 t-test). Data presented as mean ± SEM.

In theory, the maintenance of normal GABA/AMPA ratio in PSD-93 KO can be accomplished by a multiplicity of different mechanisms. For example, PSD-93 deletion can result in increased AMPAR neurotransmission also in inhibitory neurons, an idea reinforced by the expression of PSD-93 in this cell type. Alternatively, GABAergic input could be homeostatically up regulated in order to maintain a physiological level of intracortical inhibition, when compared to excitation. This homeostatic up regulation can be expressed as increases in the excitability of interneurons, number of GABAergic synapses, release of GABA and others. Additional experiments with direct comparison of $GABA_A$ IPSCs and NMDA EPSCs will further confirm whether PSD-93 deletion affects GABAergic neurotransmission.

3.12 Impaired LTD in the absence of PSD-93.

Synaptic plasticity is the ability of synapses to strengthen or weaken in response to changes in their activity (Hughes, 1958). Several mechanisms are involved, including changes in the efficiency of postsynaptic response or alterations in neurotransmitter release. Long-term potentiation (LTP) and long-term depression (LTD) refer to synaptic strengthening and weakening, respectively. PSD-93 deletion has no effect on basal NMDAR neurotransmission in hippocampus; however it impairs NMDAR-dependent LTP in this that brain region (Carlisle et al, 2008). Therefore, to check whether PSD-93 also plays a role in visual cortex, NMDAR-dependent synaptic plasticity was evaluated in L4-L2/3 synapses of PSD-93 KO slices at PD21-30.

Previous work on acute slices show that Low Frequency induced LTD at L4-L2/3 synapses relies on the integrity of postsynaptic NMDARs (Crozier et al, 2007).

In Control slices LTD was successfully induced by pairing postsynaptic depolarization to -45 mV (100 ms) with presynaptic stimulation of L4/L2-3 synapses at 1Hz for 5 min (Fig. 3.14 and 3.15; Control 63.9% ± 6.1 [n/m = 7/5]). Consistent with previous reports, L4-L2/3 LTD relied on NMDARs, as LTD could not be reliably induced in the presence of NMDAR blocker APV 100μM (Fig 3.14B-F; Control + APV, 90.5% ± 8.4 [n/m = 4/6]).

In thalamocortical and hippocampus synapses, NMDAR-dependent LTD requires PKA activation and clathrin-dependent endocytosis of postsynaptic AMPARs. Thus, synaptic weakening is achieved through reduced postsynaptic response to glutamate. In L4-L2/3 synapses, NMDAR-dependent LTD is blocked by CB1-cannabinoid receptor (CB1R) antagonists but not by inhibitors of PKA or clathrin-dependent AMPAR endocytosis (Crozier et al, 2007). It is suggested that endocannabinoids released by the postsynaptic neuron, in a calcium dependent manner, diffuse along the synaptic cleft to activate presynaptic CB1Rs and induce LTD (Sjöstrom et al, 2003). Thus, synaptic weakening is proposed to be achieved through reduction in glutamate release.

Again, consistent with previous reports, blockade of CB1Rs by AM-251 2μM prevented LTD induction in acute slices (Fig 3.14C-F; Control + AM-251, 93.3% ± 7.5 [n/m = 4/2]).

Furthermore, the LTD protocol induced AMPAR EPSC potentiation, instead of depression, in PSD-93 KO slices (Fig 3.14D-F; PSD-93 KO, 146% ± 5.8 [n/m = 4/4]). Experiments performed in the presence of APV 100μM showed that NMDAR antagonism blocks the potentiation caused by PSD-93 deletion (Fig 3.14D-F; PSD-93 KO + APV, 94.6 ± 10.1 [n/m = 5/3]).

PSD-93 does not regulate basal NMDAR neurotransmission; however it plays a key role in regulating NMDAR-dependent synaptic plasticity at L4-L2/3 synapses. This result evidences a function of PSD-93 in regulating NMDAR-associated downstream signaling pathways which play a physiological role in modulating the strength of glutamatergic synapses through synaptic plasticity mechanisms.
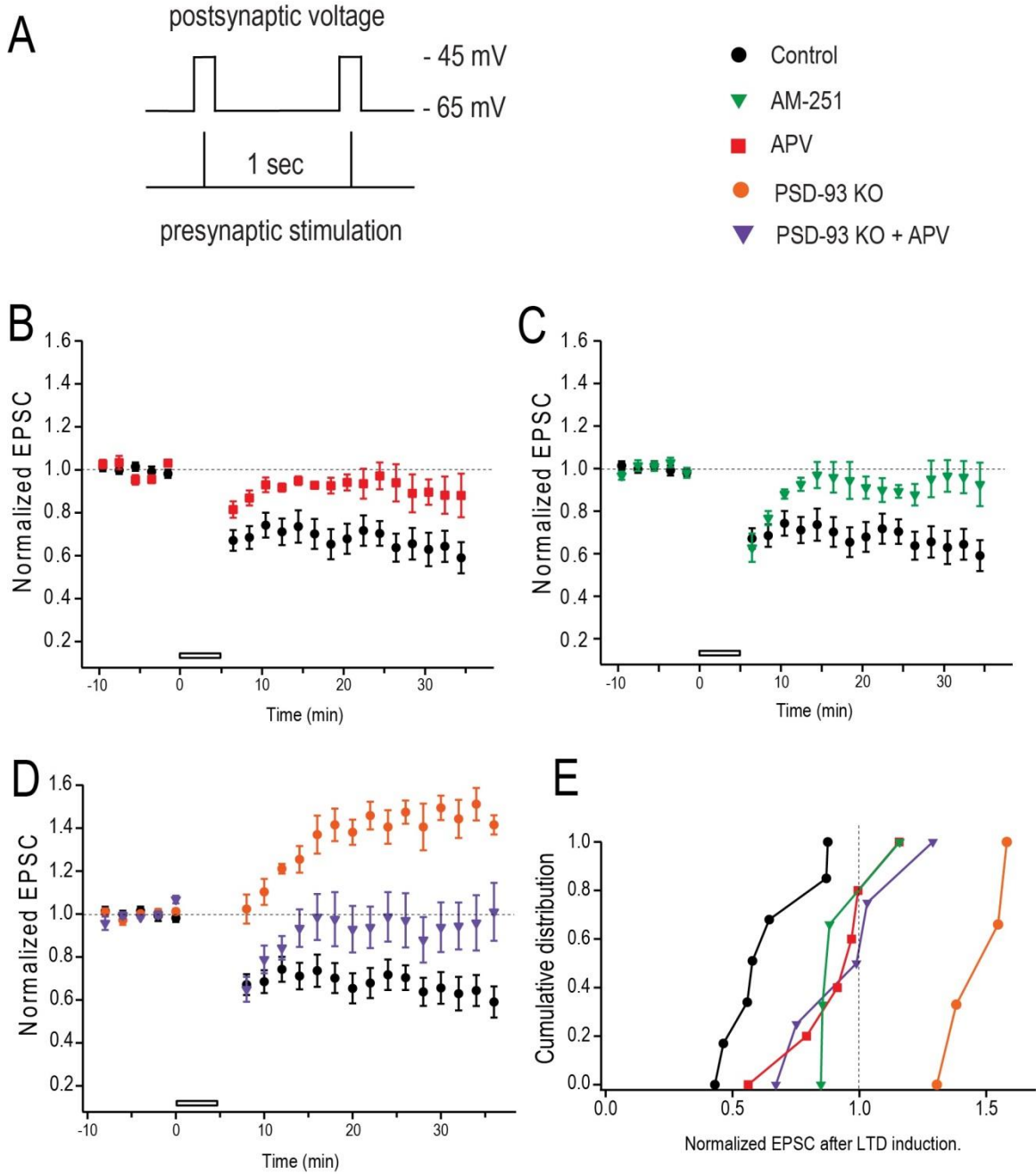
Figure 3. 14 (previous page and this page): Impaired LTD in PSD-93 KO mice.
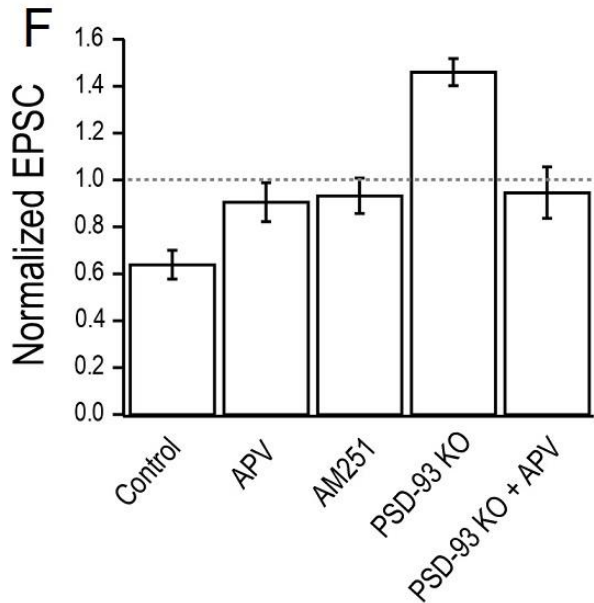
A: scheme of pairing protocol to induce LTD, postsynaptic depolarization to -45 mV was paired with presynaptic stimulation at 1 Hz for 5 min. LTD was induced after 10 min of stable baseline recording. **B-D**: Summary traces of LTD in Control (B-D, black circles), Control + NMDAR blocker APV 100μM (B, red circles); Control + CB1R blocker AM-251 2μM (C, green circles); PSD-93 KO (D, orange circles), and PSD-93 KO + NMDAR blocker APV 100μM (D, purple circles). **E:** Cumulative distribution of EPSC amplitudes 25-30 min after LTD induction normalized to initial EPSC amplitude. **F**: Summary bar graph showing EPSC amplitudes 25-30 min after LTD induction normalized to initial EPSC amplitude for each group (Control vs. APV, $p<0.05$; Control vs. AM251, $p<0.05$; Control vs. PSD-93 KO, $p<0.05$; Control vs. PSD-93 KO + APV, $p<0.05$; PSD-93 KO vs. APV, $p<0.05$; PSD-93 KO vs. AM251; $p<0.05$; PSD-93 KO vs. PSD-93 KO + APV, $p<0.05$; t-test). Data presented as mean ± SEM.

4 Environmental enrichment preserves juvenile-like levels of intracortical inhibition throughout adulthood.

In visual cortex, ocular dominance plasticity (ODP), induced by monocular deprivation (MD), declines during development and is absent in adulthood, after PD110. However, by raising mice in an enriched environment (EE) with enhanced social, physical and cognitive stimulation, ODP was preserved and reliably induced beyond PD130 (Greifzu et al, 2014).

In order to dissect the synaptic changes underlying preserved brain plasticity in EE at PD>130, brain slices from mice raised in EE and standard cages (SC) were prepared. Extracellular stimulation was delivered at L4 and synaptic responses (EPSCs and IPSCs) recorded from L2/3 neurons using the voltage-clamp configuration.

4.1 Normal AMPA/NMDA ratio in EE mice.

To evaluate whether EE affects basal glutamatergic neurotransmission, AMPAR EPSCs were recorded at -60mV and late NMDAR EPSCs were recorded at +40mV (Fig. 4.1A). In agreement with the idea that AMPARs are gradually added to postsynaptic sites during development, there is a selective increase in AMPAR EPSCs to NMDAR EPSCs in adult SC mice at PD>130 (SC) compared to juvenile SC mice at PD21-30 (SC juvenile). EE mice at PD>130 showed similar AMPA/NMDA ratio when compared to age-matched SC mice. (Fig. 4.1A-B; SC juvenile, 1.61 ± 0.15 [n/m = 13/4]; SC, 2.37 ± 0.29 [n/m = 21/5]; EE, 2.37 ± 0.19 [n/m = 17/9]).

The results suggest that increases in AMPAR EPSCs to NMDAR EPSCs at excitatory synapses are a signature of normal brain development. Both EE and SC synapses present similar AMPA/NMDA ratio at PD<130, indicating that changes in basal glutamatergic neurotransmission do not contribute to the preserved brain plasticity of EE mice.
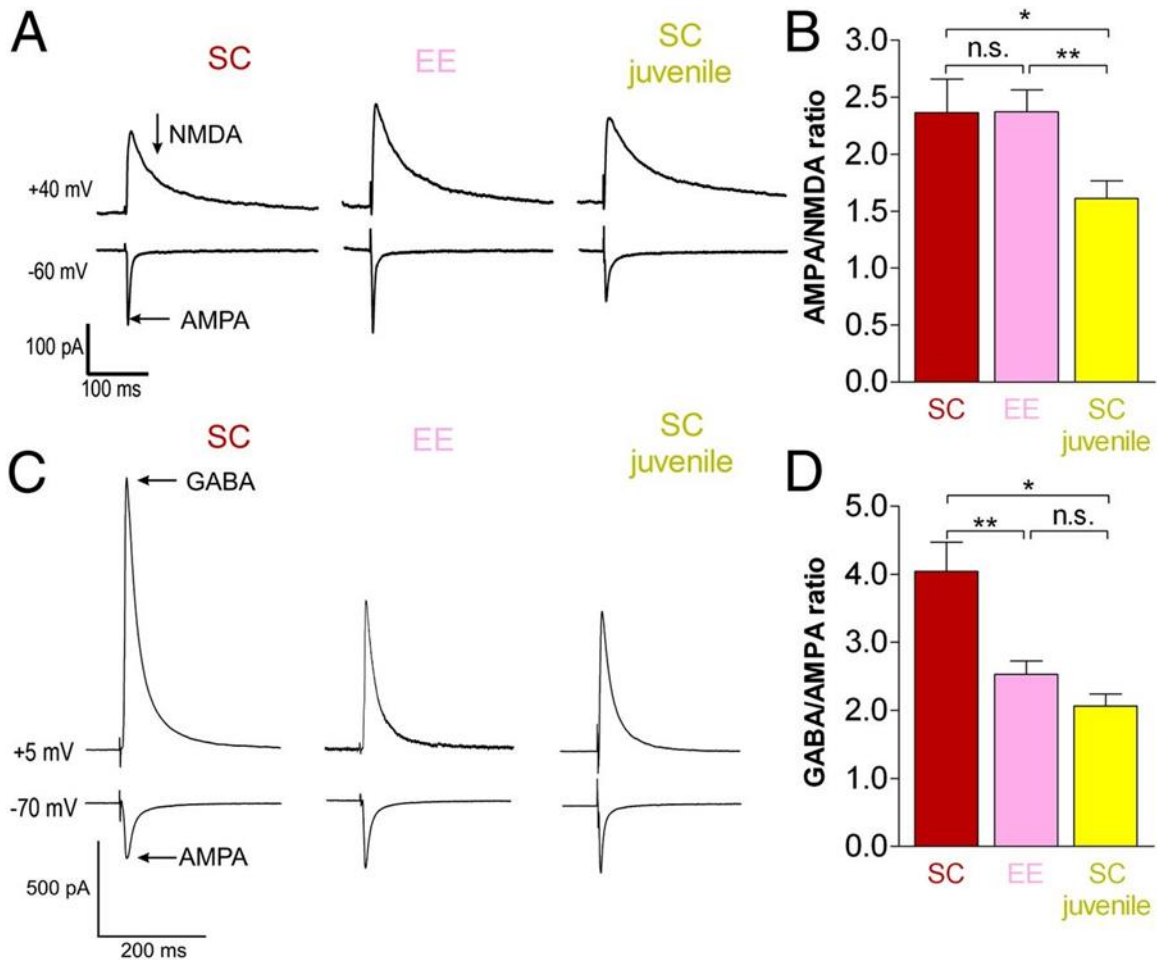
Figure 4. 1: Environmental enrichment preserves juvenile-like levels of intracortical inhibition throughout adulthood.

A: Sample average traces of AMPA/NMDA ratio recordings in slices from SC, EE and SC juvenile mice. AMPAR EPSC is the peak value at -60 mV; late NMDAR EPSC was recorded 60 ms after AMPAR peak, at +40 mV. Inhibition was blocked by picrotoxin 50μM. **B**: Summary bar graph of AMPA/NMDA ratio results (SC vs. SC juvenile, p<0.05; EE vs. SC juvenile, P<0.01; t-test). **C:** representative average AMPAR EPSCs recorded at -70mV (reversal potential of GABA$_A$), and average GABA$_A$ IPSCs recorded at +5mV (reversal potential of AMPAR). NMDARs were blocked by APV 50μM. **D**: Summary bar graph of GABA/AMPA ratio results (SC vs. SC juvenile, p<0.05; SC vs. EE, p<0.01; t-test). Data presented as mean ± SEM.

4.2 Juvenile-like levels of inhibition in adult EE mice.

Inhibitory GABAergic interneurons are key elements regulating the activity of local cortical circuits. Consistent with this notion, the preserved cortical plasticity

observed in EE mice at PD>130 can be partially abolished by boosting GABAergic neurotransmission with diazepam (Greifzu *et al*, 2014), suggesting intracortical inhibition to be a key factor modulating this form of brain plasticity.

In order to evaluate inhibitory tone directly, isolated $GABA_A$ IPSCs were recorded at +5mV (reversal potential for AMPARs), and AMPAR EPSCs were recorded at -70 mV (reversal potential for $GABA_A$). NMDARs were continuously blocked by APV 50μM. GABA/AMPA ratio was defined as $GABA_A$ IPSC amplitude normalized to AMPAR EPSC amplitude.

The GABA/AMPA ratio was robustly increased in adult SC mice at PD>130 (SC) when compared to juvenile SC mice at PD21-30 (SC juvenile), suggesting that, during normal development, intracortical inhibition increases in a higher rate when compared to AMPAR neurotransmission. In adult EE mice at PD>130 the GABA/AMPA ratio was indistinguishable from juvenile mice, evidencing that environmental enrichment preserves a juvenile-like level of inhibition/excitation ratio throughout adulthood. (Fig. 4.1B-C; SC juvenile, 2.07 ± 0.17 [n/m = 18/3]; SC, 4.04 ± 0.43 [n/m = 12/3]; EE, 2.53 ± 0.20 [n/m = 16/3]).

Taken together, the results point out that environmental enrichment preserves a juvenile-like inhibitory tone into adulthood without affecting basal excitatory glutamatergic neurotransmission.

5 Discussion

5.1 Maturation of glutamatergic synapses in visual cortex.

In visual cortex, the normal maturation of L4-L2/3 glutamatergic synapses was characterized by a robust reduction in the fraction of silent synapses: from 80% at PD3-5 to about 25% at PD21-30 (Fig. 3.10). Generally, silent synapses which exhibit functional postsynaptic NMDARs, but not AMPARs, are observed at the initial periods of synaptogenesis. During further development, they are converted into functional ones by gradual insertion and stabilization of AMPARs at the postsynaptic site (Rumpel et al, 1998).

Silent synapses exhibit NMDAR EPSCs at positive membrane potentials, but not at hyperpolarized potentials due to voltage-dependent blockade of NMDARs by extracellular magnesium. In contrast, AMPAR EPSCs are undetectable. Thus, at resting membrane potentials silent synapses present no EPSCs following neurotransmitter release and are considered functionally silent (Isaac et al, 1995; Liao et al, 1995).

Consistent with this notion, in visual cortex failure analysis of unitary EPSCs systematically showed higher EPSC failure rates at -60mV when compared to +40mV (Fig 3.10). In case both AMPARs and NMDARs were co localized at postsynaptic sites, the failure rates at different potentials should be indistinguishable. Thus, the present results suggest the existence of silent synapses, which contain only NMDARs at the postsynaptic site. Furthermore, silent synapses were directly confirmed by observing pure NMDAR EPSCs at +40mV and no AMPAR EPSCs at -60mV in some L2/3 neurons at PD3-5 (Fig. 3.10A).

Interestingly, in the rat it was reported that the fraction of silent synapses was initially very low in L2/3 neurons; it increased up to 50% around PD12 and then gradually decreased during further development. This finding was considered to be an exception to the notion that silent synapses decrease and not increase, during development (Rumpel et al, 2004). Furthermore, the same study showed that in L4 the fraction of silent synapses was initially very high, and then decreased during normal

development. In this context, the present findings in mice, involving analysis of silent synapses in 29 L2/3neurons (fig 3.10-3.11), are similar to the findings in L4 neurons of rats.

5.2   PSD-93 deletion accelerates synaptic maturation.

Gradual decreases in the fraction of silent synapses are a signature of normal brain development. However, the molecular and cellular mechanisms underlying this process are poorly understood.

Currently, the dominant view suggests that AMPARs are added to silent synapses in an activity-dependent manner, requiring NMDAR activation in an LTP-like fashion (Isaac et al, 1995, 1997; Liao et al, 1995; Durand et al, 1996, Rumpel et al, 1998). Thus, normal synaptic maturation relies on a proper functional interplay between NMDAR-activity and AMPAR trafficking. In this context, DLG-MAGUKs are supposed to present key functions given their potential ability to control the trafficking and membrane expression of both AMPARs and NMDARs and their critical roles governing NMDAR-dependent plasticity (Stein et al, 2003; Cuthbert et al, 2007; Carlisle et al, 2008).

Consistent with this notion, PSD-93 and PSD-95 were identified as key scaffolds orchestrating the proper maturation of AMPAR neurotransmission in the developing visual cortex (Fig 3.11).

PSD-93 deletion caused accelerated maturation of L4-L2/3 synapses (Fig. 3.11). The percentage of silent synapses was precociously decreased at PD10-12, and also at PD21-30. Furthermore, at PD21-30 EPSC failure rates at -60mV and +40 mV were indistinguishable, reflecting the complete absence of silent synapses in PSD-93 KOs. In contrast, PD3-5 synapses were normal, consistent with previous reports showing that PSD-93 is not reliably expressed before PD10 (Sans et al, 2000).

In depth electrophysiological analysis revealed that the accelerated synaptic maturation, represented by absence of silent synapses at PD21-30, caused a functional increase in the strength of AMPAR neurotransmission at L4-L2/3 synapses (Fig. 3.9). Such increases were not influenced by changes in neurotransmitter release (Fig 3.5 and 3.6), subunit composition of AMPARs (Fig. 3.8) or number/conductance of AMPARs at

existing synapses (Fig 3.4 and 3.7). Furthermore, PSD-93 deletion caused no additional effect on basal NMDAR neurotransmission at PD21-30 (Fig. 3.2 and 3.3).

Thus, PSD-93 has a specific role orchestrating the proper insertion and stabilization of AMPAR at postsynaptic sites synaptic development.

As PSD-93 starts to be expressed around PD-10, the fraction of silent synapses at PD3-5 was not affected by its deletion. Furthermore, as synapses mature faster in the absence of PSD-93, the present results suggest that endogenous PSD-93 plays an important role preventing precocious synaptic maturation in visual cortex.

5.3   PSD-93 and PSD-95 play opposite roles governing synaptic maturation.

The functional relationship between PSD-95 and AMPARs appears to be widely consistent. PSD-95 levels are directly related to the strength of AMPAR neurotransmission (Stein et al, 2003; Beique and Andrade, 2003; Beique et al, 2006; Schlüter et al, 2006). This notion was further confirmed in the present study. While PSD-95 deletion had no role at PD10-12, likely due to its poor expression at this age range, it caused reduced AMPAR neurotransmission at PD21-30 (Fig. 3.11). During normal development, the percentage of silent synapses decreased from about 50% at PD10-12, just before eye opening, to about 25% at PD21-30. In contrast, the fraction of silent synapses remained about 50% at PD21-30 in the absence of PSD-95. Consistent with the present data, PSD-95 overexpression strengthens AMPAR neurotransmission and reduces the fraction of silent synapses in neocortex (Beique and Andrade, 2003).

Therefore, PSD-95 presents a role promoting synaptic maturation and stabilization of AMPAR at postsynaptic sites. In contrast, endogenous PSD-93, to some extent, counteracts synaptic maturation.

Thus, a novel and unexpected scenario appears to emerge: The idea that PSD-93 and PSD-95 present opposite functions concerning synaptic maturation and AMPAR trafficking. This idea was further analyzed by measuring silent synapses in the absence of both PSD-93 and PSD-95. As expected, PSD-93/95 double deletion rendered the fraction of silent synapses at L4-L2/3 connections indistinguishable from Control (Fig. 3.11).

These results expand the knowledge about the molecular mechanisms underlying synaptic maturation in visual cortex; and enrich the current view concerning the roles of DLG-MAGUKs and their functional interactions. As commented earlier, PSD-93 deletion was suggested to play a similar role, when compared to PSD-95, reducing AMPAR neurotransmission at hippocampus synapses (Elias et al 2006, Elias and Nicoll, 2007). However, further studies did not detect the same strong role of endogenous PSD-93 (Carlisle et al, 2008; Krüger et al, 2013). For these reasons, PSD-93 has been viewed as a minor player in the DLG-MAGUK family, having a redundant role when compared to PSD-95 concerning AMPAR basal synaptic transmission.

The present study on cortical synapses suggests that the aforementioned notion, based in hippocampus studies, cannot be generally accepted. In cortical synapses PSD-93 opposes, not mimics, PSD-95. Both DLG-MAGUKs differentially regulate the strength of AMPAR neurotransmission during synaptic development.

5.4   NMDAR-dependent modulation of silent synapses.

In vitro, silent synapses can be converted to functional synapses by induction of NMDAR-dependent LTP (Isaac et al, 1995, 1997; Liao et al, 1995; Durand et al, 1996). In this context, the specific molecular mechanisms and signaling pathways mediating the functional interplay between NMDAR activity and AMPAR trafficking to the synapses are not fully established. It is suggested that activation of CaMKII by NMDAR-mediated calcium influx can trigger AMPAR modifications during synapse unsilencing (Shirke and Malinow, 1997). As an example, expression of constitutively active CaMKII in frog tectal neurons caused accelerated AMPAR trafficking to silent synapses, promoting precocious synaptic maturation (Wu et al, 1996). Additionally, NMDAR-dependent LTP can promote CaMKII-dependent phosphorylation of AMPARs as an additional mechanism to control its trafficking (Barria et al, 1997). Therefore, PSD-93 and PSD-95 can be key players coupling NMDAR activity to downstream signaling pathways necessary for proper insertion and stabilization of synaptic AMPARs. Although the specific molecular mechanisms are unclear, the present work suggests that PSD-93 couples NMDARs to signaling mechanisms facilitating LTD, while PSD-95 couples

NMDAR activity to signaling pathways which promote the insertion and stabilization of synaptic AMPARs.

5.5 Experience-driven maturation of silent synapses.

The fraction of silent synapses gradually decreases during normal development of visual cortex. It is suggested that this process involves NMDAR-dependent insertion of AMPARs at postsynaptic sites, in an LTP-like manner (Rumpel et al, 1998). Furthermore, just before eye-opening 50% of the synapses are silent. After eye-opening, the gradual stabilization of AMPAR at postsynaptic sites is strongly driven by visual experience. As an example, if rodents are dark-reared, synaptic maturation fails to occur at L2/3 neurons and the strength of AMPAR neurotransmission (i.e fraction of silent synapses) remains similar to the observed before eye-opening (Funahashi et al, 2013).

Interestingly, the present work shows that PSD-95 deletion prevents experience-driven synaptic maturation, which takes place after PD10-12 (Fig. 3.11). In contrast, at PD10-12 just before eye-opening, PSD-95 deletion did not affect the fraction of silent synapses, reinforcing the notion that endogenous PSD-95 might be selectively involved in mediating experience-driven synaptic maturation.

The complexity of this scenario is further revealed by the fact that PSD-93 deletion already promoted accelerated synaptic maturation at PD10-12 (Fig. 3.11), before eye-opening. Therefore, if PSD-93 is merely opposing PSD-95, it is puzzling why PSD-93 deletion already affects synaptic transmission before eye-opening, when endogenous PSD-95 had no detectable effect. One possible explanation is that before eye-opening the maturation signals provided by visual experience are still too weak, so endogenous PSD-93 effectively prevents any experience-driven AMPAR insertion into the developing synapses. However, in the absence of PSD-93 the weak signals can be, to some extent, already enough to promote synaptic unsilencing. To clarify this scenario, it will be necessary to raise PSD-93 KO mice in an environment with no visual stimulation (dark-rearing). In case PSD-93 is specifically opposing experience-driven maturation, the percentage of silent synapses should stay 50% at PD10-12 and also at PD21-30, as described for dark-reared animals in previous studies (Funahashi et al, 2013).

5.6 Basal NMDAR neurotransmission does not require PSD-93.

PSD-93 deletion is reported to decrease cell-surface expression of both GluN2A and GluN2B subunits of NMDARs in spinal cord and forebrain (Tao et al, 2003; Liaw et al, 2008), and reduce NMDAR-mediated toxicity in cortical cultures (Zhang et al, 2010). In contrast, AMPAR cell-surface expression was reported to be unaffected.

At a first glance the mentioned reports appear to contradict the present results, which show normal NMDAR EPSCs in the absence of PSD-93 at PD21-30 (Fig. 3.2 and 3.3) and increased AMPAR neurotransmission at PD21-30 (Fig. 3.4, 3.9 and 3.11). However, several factors might contribute to explain these apparently discrepant results.

First, the biochemical method used to evaluate NMDAR cell-surface expression involved biotin labeling of membrane receptors, followed by quantitative western blotting. While this approach is powerful for analyzing cell-surface expression, it is not able to differentiate between synaptic and extra-synaptic NMDARs, as both, in principle, are similarly biotinilated. In contrast, the electrophysiological approaches used in the present study are selective to evaluate synaptic NMDARs. Therefore, PSD-93 deletion might have a selective effect disrupting cell-surface expression of extra-synaptic NMDARs, while synaptic NMDARs stay unchanged.

Additionally, NMDAR-dependent neurotoxicity, reported to be impaired in the absence of PSD-93, is suggested to rely on extra-synaptic NMDARs, while synaptic NMDARs appear to have an apparent protective role (Parsons and Raymond, 2014). Thus, reduced NMDAR surface expression and blunted NMDAR-mediated toxicity can be fully explained by selective changes in the function of extra-synaptic receptors.

5.7 NMDAR-dependent plasticity requires PSD-93.

Basal NMDAR neurotransmission at L4-L2/3 synapses was not affected by PSD-93 deletion. However, PSD-93 directly binds to both GluN2A and GluN2B subunits of NMDARs and, therefore, can play a role regulating the functional coupling between NMDAR activity and subsequent regulation of intracellular signaling mechanisms, including the ones related to synaptic plasticity (Carlisle et al, 2008; Liaw et al, 2008).

Consistent with this notion, PSD-93 deletion impaired NMDAR-dependent LTD in L4-L2/3 synapses (Fig 3.14). PSD-93 deletion resulted in NMDAR-dependent synaptic strengthening, and not weakening, following LTD induction. In contrast, NMDAR-dependent LTD was normal, while NMDAR-dependent LTP was blunted in PSD-93-deficient hippocampus (Carlisle et al, 2008).

Thus, PSD-93 deletion does not affect NMDAR-dependent LTD in hippocampus, but disrupts NMDAR-dependent LTD in L4-L2/3 connections of visual cortex. In this context it is important to emphasize that hippocampus LTD is mechanistically different from L4-L2/3 LTD. In hippocampus, NMDAR-dependent LTD requires PKA activation and clathrin-dependent endocytosis of postsynaptic AMPARs (Malenka and Bear, 2004). In L4-L2/3, NMDAR-dependent LTD does not involve AMPAR endocytosis, but requires endocannabinoids which are suggested to diffuse from the postsynaptic neuron to activate presynaptic CB1Rs and reduce glutamate release (Crozier et al, 2007). It is not known whether lateral diffusion of AMPARs to perisynaptic sites might play an additional role.

Although the underlying molecular alterations responsible for the changes in NMDAR-dependent LTD induction in PSD-93 deficient mice remain to be identified, the present results, in L4-L2/3 synapses, suggest that endogenous PSD-93 is responsible for coupling NMDARs to signaling molecules that facilitate LTD induction.

At the network level, NMDAR-LTD at L4-L2/3 synapses is suggested to be an important, however not unique, mechanism underlying ODP during the critical period (Heynen et al, 2003; Crozier et al, 2007). As PSD-93 KO mice exhibit disrupted LTD at PD21-30, during the critical period for ODP, it is possible that ODP might be also compromised. In this scenario, the present results, combined with further studies involving monocular deprivation in PSD-93 KO mice, might enhance the current knowledge by revealing PSD-93 as an additional player regulating synaptic plasticity and ODP in visual cortex.

Concerning the maturation of silent synapses, NMDAR-activation is suggested to promote the gradual increase of AMPARs into synapses during development. PSD-93 deletion facilitated insertion of AMPAR into synapses during development (fig 3.11), and blocked NMDAR-dependent LTD, converting it into LTP. Thus, PSD-93 deletion

facilitates the strengthening of AMPAR neurotransmission in two different conditions. This suggests that endogenous PSD-93 might have an inhibitory role preventing the NMDAR-dependent insertion and stabilization of AMPARs at postsynaptic sites. Therefore, PSD-93 does not affect basal NMDAR neurotransmission, but appears to have a key role coupling NMDAR activity to downstream signaling pathways involved in synaptic maturation and synaptic plasticity. Future studies should address whether the similar NMDAR-associated downstream mechanisms are involved in both synaptic maturation and synaptic plasticity. The involvement of PSD-93 in both scenarios suggests that this can potentially be the case.

5.8   EE influences the maturation of inhibitory neurotransmission in visual cortex.

Raising mice in EE from birth preserved ODP throughout adulthood (Greifzu et al, 2014). Electrophysiological analysis showed that EE prevented maturation of GABAergic neurotransmission, so the intracortical inhibition levels of adult EE mice (PD>130) remained low and indistinguishable from PD21-30 mice (Fig 4.1).

EE did not affect the number of Parvalbumin positive GABAergic interneurons (Greifzu et al, 2014), suggesting that the decreased inhibition might be specifically caused by functional changes in the cortical circuits. However, the abundance of other inhibitory interneurons was not analyzed.

GABA$_A$ IPSCs were evoked in L2/3 neurons by extracellular stimulation delivered to L4. In this recording configuration it is estimated that, on average, 70% of GABA$_A$ IPSCs rely on AMPAR neurotransmission into inhibitory interneurons (Huang, 2014). Therefore, the reduced inhibition observed in EE mice can be caused by a multiplicity of different mechanisms.

For example, EE can reduce AMPAR neurotransmission at inhibitory neurons, reducing their activity and consequently affecting GABA release. This hypothesis will be clarified by measuring AMPAR EPSCs directly at inhibitory neurons.

Additionally, EE can reduce intracortical inhibition by decreasing the intrinsic excitability of interneurons, a feature which can be directly assessed with whole-cell current-clamp electrophysiology. Lastly, reduced inhibitory tone can be the result of

altered GABAergic neurotransmission. This scenario will be further clarified through analysis of $GABA_A$ mIPSCs in L2/3 pyramidal neurons. Changes in mIPSC frequency or amplitude will suggest alterations in GABA release or postsynaptic $GABA_A$ function, respectively.

Once the reduced GABAergic function is fully characterized, the following step will be to define how reduced inhibition facilitates ODP in EE mice. Addressing this issue will be more challenging, as the crucial questions concerning the fundamental mechanisms of ODP remain open. The specific contribution of changes in excitatory or inhibitory neurotransmission, mediating ODP, is in dispute for more than 30 years (Smith and Bear, 2010; Espinoza and Stryker, 2012).

6   References

Akgul G, Wollmuth LP (2010). Expression pattern of membrane-associated guanylate kinases in interneurons of the visual cortex. The Journal of Comparative Neurology 518(24):4842-54.

Armstrong N, Jasti J, Beich-Frandsen M, Gouaux E (2006). Measurement of conformational changes accompanying desensitization in an ionotropic glutamate receptor. Cell 127(1):85-97.

Artola A, Hensch T, Singer W (1996). Calcium-induced long-term depression in the visual cortex of the rat in vitro. Journal of Neurophysiology 76(2):984-94.

Baroncelli L, Sale A, Viegi A, Maya Vetencourt JF, De Pasquale R, Baldini S, Maffei L (2010). Experience-dependent reactivation of ocular dominance plasticity in the adult visual cortex. Experimental Neurology 226(1):100-9.

Barria A, Muller D, Derkach V, Griffith LC, Soderling TR (1997). Regulatory phosphorylation of AMPA-type glutamate receptors by CaM-KII during long-term potentiation. Science 276(5321):2042-5.

Bear MF, Kleinschmidt A, Gu QA, Singer W (1990). Disruption of experience-dependent synaptic modifications in striate cortex by infusion of an NMDA receptor antagonist. The Journal of Neuroscience 10(3):909-25.

Béïque JC, Andrade R (2003). PSD-95 regulates synaptic transmission and plasticity in rat cerebral cortex. The Journal of Physiology 546(Pt 3):859-67.

Béïque JC, Lin DT, Kang MG, Aizawa H, Takamiya K, Huganir RL. Synapse-specific regulation of AMPA receptor function by PSD-95 (2006). Proceedings of the National Academy of Sciences USA 103(51):19535-40.

Bliss TV, Gardner-Medwin AR (1973). Long-lasting potentiation of synaptic transmission in the dentate area of the unanaestetized rabbit following stimulation of the perforant path. The Journal of Physiology 232(2):357-74.

Bonnet SA, Akad DS, Samaddar T, Liu Y, Huang X, Dong Y, Schlüter OM (2013). Synaptic state-dependent functional interplay between postsynaptic density-95 and synapse-associated protein 102. The Journal of Neuroscience 33(33):13398-409.

References

Bredt DS, Nicoll RA (2003). AMPA receptor trafficking at excitatory synapses. Neuron 40(2):361-79.

Burgard EC, Hablitz JJ (1993). NMDA receptor-mediated components of miniature excitatory synaptic currents in developing rat neocortex. Journal of Neurophysiology 70(5):1841-52.

Burkhalter A, Gonchar Y, Mellor RL, Nerbonne JM (2006). Differential expression of I(A) channel subunits Kv4.2 and Kv4.3 in mouse visual cortical neurons and synapses. The Journal of Neuroscience (26): 12274-82.

Carlisle HJ1, Fink AE, Grant SG, O'Dell TJ (2008). Opposing effects of PSD-93 and PSD-95 on long-term potentiation and spike timing-dependent plasticity. The Journal of Physiology 586:5885-900.

Carroll RC, Beattie EC, von Zastrow M, Malenka RC (2001). Role of AMPA receptor endocytosis in synaptic plasticity. Nature Reviews Neuroscience 2(5):315-24.

Carulli D, Pizzorusso T, Kwok JC, Putignano E, Poli A, Forostyak S, Andrews MR, Deepa SS, Glant TT, Fawcett JW (2010). Animals lacking link protein have attenuated perineuronal nets and persistent plasticity. Brain 133(Pt 8):2331-47.

Colquhoun D, Sivilotti LG (2004). Function and structure in glycine receptors and some of their relatives. Trends in Neuroscience 27(6): 337–44.

Crair MC, Malenka RC (1995). A critical period for long-term potentiation at thalamocortical synapses. Nature 375(6529):325-8.

Crozier RA, Wang Y, Liu CH, Bear MF (2007). Deprivation-induced synaptic depression by distinct mechanisms in different layers of mouse visual cortex. Proceedings of the National Academy of Sciences USA 104(4):1383-8.

Cuthbert PC, Stanford LE, Coba MP, Ainge JA, Fink AE, Opazo P, Delgado JY, Komiyama NH, O'Dell TJ, Grant SG (2007). Synapse-associated protein 102/dlgh3 couples the NMDA receptor to specific plasticity pathways and learning strategies. The Journal of Neuroscience 27(10):2673-82.

Dobrunz LE, Stevens CF (1997). Heterogeneity of release probability, facilitation, and depletion at central synapses. Neuron 18(6):995-1008.

Dräger UC (1975). Receptive fields of single cells and topography in mouse visual cortex. The Journal of Comparative Neurology 160(3):269-90.

Durand GM, Kovalchuk Y, Konnerth A (1996). Long-term potentiation and functional synapse induction in developing hippocampus. Nature 381(6577):71-5.

Ehrlich I, Malinow R (2004). Postsynaptic density 95 controls AMPA receptor incorporation during long-term potentiation and experience-driven synaptic plasticity. The Journal of Neuroscience 24(4):916-27.

Elias GM, Funke L, Stein V, Grant SG, Bredt DS, Nicoll RA (2006). Synapse-specific and developmentally regulated targeting of AMPA receptors by a family of MAGUK scaffolding proteins. Neuron 52(2):307-20.

Espinosa JS, Stryker MP (2012). Development and plasticity of the primary visual cortex. Neuron 75(2):230-49.

Fatt P, Katz B (1952). Spontaneous subthreshold activity at motor nerve endings. The Journal of Physiology 117(1):109-28.

Freund TF (2003). Interneuron Diversity series: Rhythm and mood in perisomatic inhibition. Trends in Neuroscience 26(9):489-95.

Funahashi R, Maruyama T, Yoshimura Y, Komatsu Y (2013). Silent synapses persist into adulthood in layer 2/3 pyramidal neurons of visual cortex in dark-reared mice. Journal of Neurophysiology 109(8):2064-76.

Giese KP, Storm JF, Reuter D, Fedorov NB, Shao LR, Leicher T, Pongs O, Silva AJ (1998). Reduced K+ channel inactivation, spike broadening, and after-hyperpolarization in Kvbeta1.1-deficient mice with impaired learning. Learning and Memory 5(4-5):257-73.

Gordon JA, Stryker MP (1996). Experience-dependent plasticity of binocular responses in the primary visual cortex of the mouse. The Journal of Neuroscience 16(10):3274-86.

Greifzu F, Pielecka-Fortuna J, Kalogeraki E, Krempler K, Favaro PD, Schlüter OM, Löwel S (2014). Environmental enrichment extends ocular dominance plasticity into adulthood and protects from stroke-induced impairments of plasticity. Proceedings of the National Academy of Sciences USA 111(3):1150-5.

62

References

Hayashi Y, Shi SH, Esteban JA, Piccini A, Poncer JC, Malinow R (2000). Driving AMPA receptors into synapses by LTP and CaMKII: requirement for GluR1 and PDZ domain interaction. Science 287(5461):2262-7.

Heine M, Groc L, Frischknecht R, Béïque JC, Lounis B, Rumbaugh G, Huganir RL, Cognet L, Choquet D (2008). Surface mobility of postsynaptic AMPARs tunes synaptic transmission. Science 320(5873):201-5.

Hessler NA, Shirke AM, Malinow R (1993). The probability of transmitter release at a mammalian central synapse. Nature 366(6455):569-72.

Heynen AJ, Yoon BJ, Liu CH, Chung HJ, Huganir RL, Bear MF (2003). Molecular mechanism for loss of visual cortical responsiveness following brief monocular deprivation. Nature Neuroscience 6(8):854-62.

Hollmann M, Heinemann S (1994). Cloned glutamate receptors. Annual Review of Neuroscience 17:31-108.

Howard MA, Elias GM, Elias LA, Swat W, Nicoll RA (2010). The role of SAP97 in synaptic glutamate receptor dynamics. Proceedings of the National Academy of Sciences USA 107(8):3805-10.

Hrabetova S, Serrano P, Blace N, Tse HW, Skifter DA, Jane DE, Monaghan DT, Sacktor TC (2000). Distinct NMDA receptor subpopulations contribute to long-term potentiation and long-term depression induction. The Journal of Neuroscience 20(12):RC81.

Huang X (2014). Role of PSD-95 in synaptic maturation and visual cortex plasticity. Georg-August-Universität Göttingen.

Huang YH, Lin Y, Mu P, Lee BR, Brown TE, Wayman G, Marie H, Liu W, Yan Z, Sorg BA, Schlüter OM, Zukin RS, Dong Y (2009). In vivo cocaine experience generates silent synapses. Neuron 63(1):40-7.

Hughes JR (1958). Post-tetanic Potentiation. Physiological Reviews 38(1): 91–113.

Isaac JT, Nicoll RA, Malenka RC (1995). Evidence for silent synapses: implications for the expression of LTP. Neuron 15(2):427-34.

Katz LC, Shatz CJ (1996). Synaptic activity and the construction of cortical circuits. Science 274(5290):1133-8.

References

Kim E, Sheng M (2004). PDZ domain proteins of synapses. Nature Reviews Neuroscience 5(10):771-81.

Kirkwood A, Silva A, Bear MF (1997). Age-dependent decrease of synaptic plasticity in the neocortex of alphaCaMKII mutant mice. Proceedings of the Nationall Academy of Sciences USA 94(7):3380-3.

Kleinschmidt A, Bear MF, Singer W (1987). Blockade of "NMDA" receptors disrupts experience-dependent plasticity of kitten striate cortex. Science 238(4825):355-8.

Kornau HC, Schenker LT, Kennedy MB, Seeburg PH (1995). Domain interaction between NMDA receptor subunits and the postsynaptic density protein PSD-95. Science 269(5231):1737-40.

Krüger JM, Favaro PD, Liu M, Kitlinska A, Huang X, Raabe M, Akad DS, Liu Y, Urlaub H, Dong Y, Xu W, Schlüter OM (2013). Differential roles of postsynaptic density-93 isoforms in regulating synaptic transmission. The Journal of Neuroscience 33(39):15504-17.

Kullmann DM, Lamsa KP (2011). Interneurons go plastic. Neuropharmacology 60(5):711.

Lehmann K, Löwel S (2008). Age-dependent ocular dominance plasticity in adult mice. PLoS One 3(9):e3120.

Leonard AS, Davare MA, Horne MC, Garner CC, Hell JW (1998). SAP97 is associated with the alpha-amino-3-hydroxy-5-methylisoxazole-4-propionic acid receptor GluR1 subunit. The Journal of Biological Chemistry 273(31):19518-24.

Liao D, Hessler NA, Malinow R (1995). Activation of postsynaptically silent synapses during pairing-induced LTP in CA1 region of hippocampal slice. Nature 375(6530):400-4.

Liaw WJ, Zhu XG, Yaster M, Johns RA, Gauda EB, Tao YX (2008). Distinct expression of synaptic NR2A and NR2B in the central nervous system and impaired morphine tolerance and physical dependence in mice deficient in postsynaptic density-93 protein. Molecular Pain 4:45.

Lin CS, Nicolelis MA, Schneider JS, Chapin JK (1990). A major direct GABAergic pathway from zona incerta to neocortex. Science 248(4962):1553-6.

Liu XB, Murray KD, Jones EG (2004). Switching of NMDA receptor 2A and 2B subunits at thalamic and cortical synapses during early postnatal development. The Journal of Neuroscience 24(40):8885-95.

Maffei A, Turrigiano GG (2008). Multiple modes of network homeostasis in visual cortical layer 2/3. The Journal of Neuroscience 28(17):4377-84.

Malenka RC, Bear MF (2004). LTP and LTD: an embarrassment of riches. Neuron 44(1):5-21.

Malenka RC, Kauer JA, Perkel DJ, Mauk MD, Kelly PT, Nicoll RA, Waxham MN (1989). An essential role for postsynaptic calmodulin and protein kinase activity in long-term potentiation. Nature 340(6234):554-7.

Malinow R, Malenka RC (2002). AMPA receptor trafficking and synaptic plasticity. Annual Review of Neuroscience 25:103-26.

Malinow R, Schulman H, Tsien RW (1989). Inhibition of postsynaptic PKC or CaMKII blocks induction but not expression of LTP. Science 245(4920):862-6.

Mangini NJ, Pearlman AL (1980). Laminar distribution of receptive field properties in the primary visual cortex of the mouse. The Journal of Comparative Neurology 193(1):203-22.

Martin IL, Dunn SMJ (2002). GABA receptors: A review of GABA and the receptors to which it binds. Tocris Cookson LTD.

Maya Vetencourt JF, Sale A, Viegi A, Baroncelli L, De Pasquale R, O'Leary OF, Castrén E, Maffei L (2008). The antidepressant fluoxetine restores plasticity in the adult visual cortex. Science 320(5874):385-8.

Mayer ML (2005). Glutamate receptor ion channels. Current Opinion in Neurobiology 15(3): 282-8.

Mayer ML, Armstrong N (2004). Structure and function of glutamate receptor ion channels. Annual Review of Physiology 66:161-81.

Mayer ML, Westbrook GL, Guthrie PB (1984). Voltage-dependent block by Mg2+ of NMDA responses in spinal cord neurones. Nature 309(5965):261-3.

McBain CJ, Fisahn A (2001). Interneurons unbound. Nature Reviews Neuroscience 2(1):11-23.

McGee AW, Topinka JR, Hashimoto K, Petralia RS, Kakizawa S, Kauer FW, Aguilera-Moreno A, Wenthold RJ, Kano M, Bredt DS (2001). PSD-93 knock-out mice reveal that neuronal MAGUKs are not required for development or function of parallel fiber synapses in cerebellum. The Journal of Neuroscience 21(9):3085-91.

Métin C, Godement P, Imbert M. The primary visual cortex in the mouse: receptive field properties and functional organization. Experimental Brain Research 69(3):594-612.

Migaud M, Charlesworth P, Dempster M, Webster LC, Watabe AM, Makhinson M, He Y, Ramsay MF, Morris RG, Morrison JH, O'Dell TJ, Grant SG (1998). Enhanced long-term potentiation and impaired learning in mice with mutant postsynaptic density-95 protein. Nature 396(6710):433-9.

Miyata S, Komatsu Y, Yoshimura Y, Taya C, Kitagawa H (2012). Persistent cortical plasticity by upregulation of chondroitin 6-sulfation. Nature Neuroscience 15(3):414-22.

Morishita H, Miwa JM, Heintz N, Hensch TK (2010). Lynx1, a cholinergic brake, limits plasticity in adult visual cortex. Science 330(6008):1238-40.

Nakagawa T, Futai K, Lashuel HA, Lo I, Okamoto K, Walz T, Hayashi Y, Sheng M (2004). Quaternary structure, protein dynamics, and synaptic function of SAP97 controlled by L27 domain interactions. Neuron 44(3):453-67.

Nakanishi S (1992). Molecular diversity of glutamate receptors and implications for brain function. Science 258(5082):597-603.

Niethammer M, Kim E, Sheng M (1996). Interaction between the C terminus of NMDA receptor subunits and multiple members of the PSD-95 family of membrane-associated guanylate kinases. The Journal of Neuroscience 16(7):2157-63.

Nowak L, Bregestovski P, Ascher P, Herbet A, Prochiantz A (1984). Magnesium gates glutamate-activated channels in mouse central neurones. Nature 307(5950):462-5.

Paoletti P, Bellone C, Zhou Q (2013). NMDA receptor subunit diversity: impact on receptor properties, synaptic plasticity and disease. Nature Reviews Neuroscience 14(6):383-400.

Parsons MP, Raymond LA (2014). Extrasynaptic NMDA receptor involvement in central nervous system disorders. Neuron 82(2):279-93.

Passafaro M, Piëch V, Sheng M (2001). Subunit-specific temporal and spatial patterns of AMPA receptor exocytosis in hippocampal neurons. Nature Neuroscience 4(9):917-26.

Rosenmund C, Clements JD, Westbrook GL (1993). Nonuniform probability of glutamate release at a hippocampal synapse. Science 262(5134):754-7.

Rosenmund C, Stern-Bach Y, Stevens CF (1998). The tetrameric structure of a glutamate receptor channel. Science 280 (5369): 1596–9.

Rumbaugh G, Sia GM, Garner CC, Huganir RL (2003). Synapse-associated protein-97 isoform-specific regulation of surface AMPA receptors and synaptic function in cultured neurons. The Journal of Neuroscience 23(11):4567-76.

Rumpel S, Hatt H, Gottmann K (1998). Silent synapses in the developing rat visual cortex: evidence for postsynaptic expression of synaptic plasticity. The Journal of Neuroscience 18(21):8863-74.

Rumpel S, Kattenstroth G, Gottmann K (2004). Silent synapses in the immature visual cortex: layer-specific developmental regulation. Journal of Neurophysiology 91(2):1097-101.

Sale A, Maya Vetencourt JF, Medini P, Cenni MC, Baroncelli L, De Pasquale R, Maffei L (2007). Environmental enrichment in adulthood promotes amblyopia recovery through a reduction of intracortical inhibition. Nature Neuroscience 10(6):679-81.

Sans N, Petralia RS, Wang YX, Blahos J, Hell JW, Wenthold RJ (20009. A developmental change in NMDA receptor-associated proteins at hippocampal synapses. The Journal of Neuroscience 20(3):1260-71.

Sattler R, Xiong Z, Lu WY, Hafner M, MacDonald JF, Tymianski M (1999). Specific coupling of NMDA receptor activation to nitric oxide neurotoxicity by PSD-95 protein. Science 284(5421):1845-8.

Scali M, Baroncelli L, Cenni MC, Sale A, Maffei L (2012). A rich environmental experience reactivates visual cortex plasticity in aged rats. Experimental Gerontology 47(4):337-41.

Schlüter OM, Xu W, Malenka RC (2006). Alternative N-terminal domains of PSD-95 and SAP97 govern activity-dependent regulation of synaptic AMPA receptor function. Neuron 51(1):99-111.

Schnell E, Sizemore M, Karimzadegan S, Chen L, Bredt DS, Nicoll RA (2002). Direct interactions between PSD-95 and stargazin control synaptic AMPA receptor number. Proceedings of the National Academy of Sciences USA 99(21):13902-7.

Sermasi E, Tropea D, Domenici L (1999). A new form of synaptic plasticity is transiently expressed in the developing rat visual cortex: a modulatory role for visual experience and brain-derived neurotrophic factor. Neuroscience 91(1):163-73.

Shirke AM, Malinow R (1997). Mechanisms of potentiation by calcium-calmodulin kinase II of postsynaptic sensitivity in rat hippocampal CA1 neurons. Journal of Neurophysiology 78(5):2682-92.

Sjöstrom PJ, Turrigiano GG, Nelson SB (2003). Neocortical LTD via coincident activation of presynaptic NMDA and cannabinoid receptors. Neuron 39(4):641-54.

Smith GB, Bear MF (2010). Bidirectional ocular dominance plasticity of inhibitory networks: recent advances and unresolved questions. Frontiers in Cellular Neuroscience 4:21.

Stein V, House DR, Bredt DS, Nicoll RA (2003). Postsynaptic density-95 mimics and occludes hippocampal long-term potentiation and enhances long-term depression. The Journal of Neuroscience 23(13):5503-6.

Suska A, Lee BR, Huang YH, Dong Y, Schlüter OM (2013). Selective presynaptic enhancement of the prefrontal cortex to nucleus accumbens pathway by cocaine. Proceedings of the National Academy of Sciences USA 110(2):713-8.

Syken J, Grandpre T, Kanold PO, Shatz CJ (2006). PirB restricts ocular-dominance plasticity in visual cortex. Science 313(5794):1795-800.

Taha S, Hanover JL, Silva AJ, Stryker MP (2002). Autophosphorylation of alphaCaMKII is required for ocular dominance plasticity. Neuron 36(3):483-91.

Tao YX, Rumbaugh G, Wang GD, Petralia RS, Zhao C, Kauer FW, Tao F, Zhuo M, Wenthold RJ, Raja SN, Huganir RL, Bredt DS, Johns RA (2003). Impaired NMDA receptor-mediated postsynaptic function and blunted NMDA receptor-dependent persistent pain in mice lacking postsynaptic density-93 protein. The Journal of Neuroscience 23(17):6703-12.

Tsien JZ, Huerta PT, Tonegawa S (19969. The essential role of hippocampal CA1 NMDA receptor-dependent synaptic plasticity in spatial memory. Cell 87(7):1327-38.

Varga AW, Yuan LL, Anderson AE, Schrader LA, Wu GY, Gatchel JR, Johnston D, Sweatt JD (2004). Calcium-calmodulin-dependent kinase II modulates Kv4.2 channel expression and upregulates neuronal A-type potassium currents. The Journal of Neuroscience (24): 3643-54.

Wagor E, Mangini NJ, Pearlman AL (1980). Retinotopic organization of striate and extrastriate visual cortex in the mouse. The Journal of Comparative Neurology 193(1):187-202.

Wang CY, Chang K, Petralia RS, Wang YX, Seabold GK, Wenthold RJ (2006). A novel family of adhesion-like molecules that interacts with the NMDA receptor. The Journal of Neuroscience 26(8):2174-83.

Wiltgen BJ, Royle GA, Gray EE, Abdipranoto A, Thangthaeng N, Jacobs N, Saab F, Tonegawa S, Heinemann SF, O'Dell TJ, Fanselow MS, Vissel B (2010). A role for calcium-permeable AMPA receptors in synaptic plasticity and learning. PLoS One 5(9).

Wu G, Malinow R, Cline HT (1996). Maturation of a central glutamatergic synapse. Science 274(5289):972-6.

Xu J, He L, Wu LG (2007). Role of Ca(2+) channels in short-term synaptic plasticity. Current Opinion in Neurobiology 17(3):352-9.

Xu W, Schlüter OM, Steiner P, Czervionke BL, Sabatini B, Malenka RC (2008). Molecular dissociation of the role of PSD-95 in regulating synaptic strength and LTD. Neuron 57(2):248-62.

Yang Y, Fischer QS, Zhang Y, Baumgärtel K, Mansuy IM, Daw NW (2005). Reversible blockade of experience-dependent plasticity by calcineurin in mouse visual cortex. Nature Neuroscience 8(6):791-6.

Yazaki-Sugiyama Y, Kang S, Câteau H, Fukai T, Hensch TK (2009). Bidirectional plasticity in fast-spiking GABA circuits by visual experience. Nature 462(7270):218-21.

Zhang M, Xu JT, Zhu X, Wang Z, Zhao X, Hua Z, Tao YX, Xu Y (2010). Postsynaptic density-93 deficiency protects cultured cortical neurons from N-methyl-D-aspartate receptor-triggered neurotoxicity. Neuroscience 166(4):1083-90.

Zucker RS, Regehr, WG (2002). Short-Term Synaptic Plasticity. Annual Review of Physiology 64: 355–405

7 Acknowledgements

I am thankful to:

- Dr. Dr. Oliver M. Schlüter, for the opportunity to conduct my Doctoral studies in his laboratory.
- To my thesis committee members: Prof. Walter Stühmer, Prof. Michael Hörner and Dr. Holger Taschenberger, for valuable input which contributed to my project.
- To Prof. Siegrid Löwel and her group, for the fruitful scientific collaborations.
- To Prof. Nils Bröse and his group, for the intellectual feedback about my project.
- To all past and present members of the Molecular Neurobiology Department at the European Neuroscience Institute Göttingen.
- To all who directly or indirectly contributed to my Doctoral studies, especially to Johanna Schulke, to my brother Felipe, my mother Dalva and my father Plinio.

8 Curriculum Vitae

Personal Data

Name	Plinio Das Neves Favaro
Date of birth	November 24th, 1986
Place of birth	Londrina, Brazil
E-mail	favaro.137@gmail.com

Education

10/2010 – 09/2014	Doctoral Studies in Molecular Physiology of the Brain.
	With Dr. Dr. Oliver M. Schlüter.
	European Neuroscience Institute, Göttingen, Germany.
	Thesis: Roles of PSD-93 and environmental enrichment in cortical synapses.
02/2008 – 07/2010	M.Sc. in Physiology.
	With Prof. Dr. Eliane Comoli.
	University of São Paulo, Ribeirão Preto, Brazil.
	Thesis: Organization of the afferent connections to the medial and lateral regions of the rat's Superior Colliculus.
03/2004 – 11/2007	B.Sc. in Biomedicine.
	With Prof. Dr. Estefânia G. Moreira.
	State University of Londrina, Londrina, Brazil.
	Thesis: Evaluation of the behavioral response to Diazepam and Diethylproprion in mice exposed to fluoxetine during pregnancy and lactation.

Scholarships

10/2014 – 12/2014	Bridging Funding GGNB, Germany.
10/2011 – 09/2014	Erasmus Mundus scholarship (ENC Network), European Comission.
10/2010 – 09/2011	GGNB scholarship, Germany.
02/2008 – 02/2010	FAPESP scholarship (State of São Paulo), Brazil.
11/2006 – 11/2007	UEL scholarship (State University of Londrina), Brazil.

Travel Grants

2014	GGNB Travel Grant
2012	GGNB Travel Grant
2010	FENS-IBRO-SfN Travel Grant

Publications

Greifzu F, Pielecka-Fortuna J, Kalogeraki E, Krempler K, **Favaro PD**, Schlüter OM, Löwel S. Environmental enrichment extends ocular dominance plasticity into adulthood and protects from stroke-induced impairments of plasticity. *Proc Natl Acad Sci U S A*. 2014 Jan 21;111(3):1150-5.

Krüger JM, **Favaro PD**, Liu M, Kitlinska A, Huang X, Raabe M, Akad DS, Liu Y, Urlaub H, Dong Y, Xu W, Schlüter OM. Differential roles of postsynaptic density-93 isoforms in regulating synaptic transmission. *J Neurosci*. 2013 Sep 25;33(39):15504-17.

Comoli E, **Favaro PD**, Vautrelle N, Leriche M, Overton PG, Redgrave P. Segregated anatomical input to sub-regions of the rodent superior colliculus associated with approach and defense. *Front Neuroanat*. 2012 Apr 3;6:9.

Favaro PD, Gouvêa TS, de Oliveira SR, Vautrelle N, Redgrave P, Comoli E. The influence of vibrissal somatosensory processing in rat superior colliculus on prey capture. *Neuroscience*. 2011 Mar 10;176:318-27.

Favaro PD, Costa LC, Moreira EG. Maternal fluoxetine treatment decreases behavioral response to dopaminergic drugs in female pups. *Neurotoxicol Teratol*. 2008 Nov-Dec;30(6):487-94.